

**ANALYZING VIDEO COMPRESSION FOR TRANSPORTING OVER  
WIRELESS FADING CHANNELS**

A Thesis

by

**KARTHIK KANNAN**

Submitted to the Office of Graduate Studies of  
Texas A&M University  
in partial fulfillment of the requirements for the degree of

**MASTER OF SCIENCE**

August 2006

Major Subject: Electrical Engineering

**ANALYZING VIDEO COMPRESSION FOR TRANSPORTING OVER  
WIRELESS FADING CHANNELS**

A Thesis

by

**KARTHIK KANNAN**

Submitted to the Office of Graduate Studies of  
Texas A&M University  
in partial fulfillment of the requirements for the degree of

**MASTER OF SCIENCE**

Approved by:

Chair of Committee,	Scott Miller
Committee Members,	Zixiang Xiong
	Shankar Bhattacharyya
	Riccardo Bettati
Head of Department,	Costas N. Georghiades

August 2006

Major Subject: Electrical Engineering

**ABSTRACT**

Analyzing Video Compression for Transporting over Wireless  
Fading Channels. (August 2006)

Karthik Kannan, B.E, Bharadhasan University, Regional Engineering College Trichy  
Chair of Advisory Committee: Dr. Scott Miller

Wireless video communication is becoming increasingly popular these days with new applications such as TV on mobile and video phones. Commercial success of these applications requires superior video quality at the receiver. So it is imperative to analyze the effect of a wireless channel on a video transmission. The aim of this research is to analyze the video transmission over Rayleigh fading channels for various bit error rates (BER), signal to noise ratios ( $E_b/N_0$ ) and Doppler rates, and to suggest which source coding scheme is best at which BER,  $E_b/N_0$  and Doppler rates. Alternative schemes such as hybrid (digital/analog) schemes were considered and their performances were compared with pure digital communication. It is also shown that the combination of digital and analog video communication does not yield any better performance compared to pure digital video communication.

**DEDICATION**

To my loving parents

## ACKNOWLEDGEMENTS

I would like to thank my committee chair, Dr. Scott Miller for his never ending support, invaluable guidance, and excellent suggestions throughout the course of this research. I also would like to thank my committee members Dr.Zixiang Xiong, Dr. Shankar Bhattacharyya and Dr.Riccardo Bettati for their support, time and efforts. I would like to thank the Head of the Electrical Engineering Department, Dr.Costas Georghiades, for providing me an opportunity to present this research.

I would like to thank the Electrical Engineering Department and Texas A&M University for providing the necessary infrastructure to carry out this research. I would like to extend my gratitude to the Internet Technology Evaluation Center (ITEC), Texas A&M University and to the Director of Telecommunication Department, Dr.Walt Magnussen, for their support.

Thanks to my parents and relatives for their continued encouragement and moral support. Finally, thanks to my roommates and friends for their needed help.

## TABLE OF CONTENTS

	Page
ABSTRACT .....	iii
DEDICATION .....	iv
ACKNOWLEDGEMENTS .....	v
TABLE OF CONTENTS .....	vi
LIST OF TABLES .....	viii
LIST OF FIGURES.....	x
 CHAPTER	
I INTRODUCTION.....	1
II BACKGROUND INFORMATION ON H.264 .....	3
A. Introduction .....	3
B. Video Standard Basics.....	3
C. H.264 Encoder .....	5
D. H.264 Decoder.....	7
E. Highlights of H.264 .....	8
III BACKGROUND INFORMATION ON RAYLEIGH FADING CHANNELS .....	10
A. Introduction .....	10
B. Power Spectrum of Rayleigh Fading Process.....	11
C. Time Domain Method .....	12
D. Important Results .....	14
IV VIDEO TRANSMISSION OVER RAYLEIGH FADING CHANNELS.....	16
A. Introduction .....	16
B. System Setup .....	18
C. RTP Packetization .....	19
D. Frame Erasure Processing .....	24
E. Experimental Results .....	32

CHAPTER	Page
V	
HYBRID SOURCE CODING FOR VIDEO TRANSMISSION OVER RAYLEIGH FADING CHANNELS .....	53
A. Introduction .....	53
B. System Setup .....	53
C. Analog Source Coding.....	54
D. Experimental Results.....	62
VI	
CONCLUSION .....	73
REFERENCES .....	75
VITA .....	78

## LIST OF TABLES

TABLE	Page
4.1	NALU Packet Structure Field Description..... 21
4.2	RTP Packet Header Field Description for H.264 ..... 22
4.3	Field Description for RTP Packet Structure for Transporting Fragmented NALU ..... 23
4.4	Common Test Conditions..... 32
4.5	Variable Test Conditions..... 32
4.6	$E_b / N_0$ - BER Relationship for Various $F_d$ ..... 33
4.7	Experiment 1 Test Conditions..... 34
4.8	Experiment 2 Test Conditions..... 36
4.9	Experiment 3 Test Conditions..... 38
4.10	Experiment 4 Test Conditions..... 39
4.11	Experiment 5 Test Conditions..... 41
4.12	Experiment 6 Test Conditions..... 42
4.13	Average $FoM$ Computed for Experiment 6 Test Conditions .... 43
4.14	Experiment 7 Test Conditions..... 45
4.15	Experiment 8 Test Conditions..... 46
4.16	Average $FoM$ Computed for Experiment 8 Test Conditions .... 47
4.17	Experiment 9 Test Conditions..... 48
4.18	Experiment 10 Test Conditions..... 51



TABLE		Page
5.1	Hybrid Coding: Common Test Conditions .....	62
5.2	Hybrid Coding: Variable Test Conditions .....	62
5.3	Hybrid Coding: Experiment 1 Test Conditions.....	63
5.4	Hybrid Coding: Experiment 2 Test Conditions.....	65
5.5	Hybrid Coding: Experiment 3 Test Conditions.....	67
5.6	Hybrid Coding: Experiment 4 Test Conditions.....	68
5.7	Bandwidth Comparison: Hybrid Beta Coding, $\beta=50\%$ vs Pure Digital Coding .....	70
5.8	Hybrid Coding: Experiment 5 Test Conditions.....	70
5.9	Bandwidth Comparison: Hybrid Coding by DCT ordering vs Pure Digital Coding .....	71

## LIST OF FIGURES

FIGURE	Page
2.1 H.264 Encoder block diagram.....	6
3.1 PSD of a Rayleigh fading process. Maximum doppler shift is 100Hz .....	12
3.2 Autocorrelation function of a Rayleigh fading process.....	13
3.3 Magnitude response of a Rayleigh fading process.....	15
3.4 Phase response of Rayleigh fading process.....	15
4.1 Wireless system setup, Transmitter.....	18
4.2 Wireless system setup, Receiver .....	19
4.3 H.264 Encoder packet layers.....	20
4.4 NALU packet structure .....	20
4.5 RTP packet structure for H.264.....	22
4.6 RTP packet structure for transporting fragmented NALU.....	23
4.7 FoM @ $F_d=10\text{Hz}$ , IDR Period=0, 6 MBs/slice for various $E_b/N_0=24\text{dB}$ to $53\text{dB}$ .....	35
4.8 Frame 1: Distortion observed in left picture ( $E_b/N_0=24\text{dB}$ ) Right picture ( $E_b/N_0=53\text{dB}$ ) is distortion free .....	35
4.9 FoM @ $E_b/N_0=37.5\text{dB}$ , IDR Period=0, 6 MBs/slice for $F_d = 10\text{Hz}, 50\text{Hz}, 100\text{Hz}$ .....	37
4.10 Frame 1. Left picture ( $F_d=50\text{Hz}$ ) is distortion free Right picture ( $F_d=100\text{Hz}$ ) has distortions.....	37
4.11 FoM @ $E_b/N_0=37.5\text{dB}, 44.5\text{dB}$ , IDR Period=0, 6 MBs/slice slice for $F_d = 10\text{Hz}, 50\text{Hz}, 100\text{Hz}$ .....	38

FIGURE	Page
4.12 FoM @ $F_d=10\text{Hz}, 50\text{Hz}, 100\text{Hz}$ , IDR Period=10, 6 MBs/slice for various $E_b/N_0=44.5\text{dB}, 53\text{dB}$ .....	40
4.13 IDR period comparison. FoM @ $F_d=50\text{Hz}$ , IDR Period=0,10, 6 MBs/slice, $E_b/N_0=37.5\text{dB}$ .....	42
4.14 FoM plot, IDR period =10 performing better @ higher valued $E_b/N_0=47.5\text{dB}$ , $F_d=50\text{Hz}$ .....	44
4.15 Frame 20, Left (IDR Period=0) has distortions . Right (IDR Period=10) is distortion free .....	44
4.16 FoM plot, Single slice/picture performance @ $E_b/N_0=37.5\text{dB}, 44.5\text{dB}, F_d=10\text{Hz}, 50\text{Hz}$ , IDR period =0.....	46
4.17 Comparison between (1) multiple slice/picture, IDR period =0 $E_b/N_0=37.5\text{dB}, F_d=50\text{Hz}$ ; (2) multiple slice/picture, IDR period =10, $E_b/N_0=44.5\text{dB}, F_d=50\text{Hz}$ ; (3) single slice/picture, IDR =0, $E_b/N_0=44.5\text{dB}, F_d=50\text{Hz}$ .....	47
4.18 Padding overhead [Kbps] is plotted against various RTP Packet Sizes .....	49
4.19 FoM for various RTP packet sizes is compared.....	49
4.20 Packet Error Rate for various $E_b/N_0$ .....	52
4.21 FoM of an informational theoretical based channel coded wireless system for a video signal transported with $E_b/N_0= 7\text{dB}, 6.5\text{dB}, 6\text{dB}, 5.5\text{dB}, 5\text{dB} \& 4\text{dB}$ .....	52
5.1 Block diagram showing the transmitter of the hybrid scheme: Beta coding of DCT coefficients.....	56
5.2 Block diagram showing the receiver of the hybrid scheme: Beta coding of DCT coefficients.....	56
5.3 Left picture (Hybrid Beta coding of DCT coefficients) & Right picture (pure Digital coding) in an error free channel.....	58
5.4 Block diagram showing the transmitter of the hybrid scheme: DCT ordering .....	60

FIGURE	Page
5.5 Block diagram showing the receiver of the hybrid scheme: DCT ordering .....	60
5.6 Hybrid Beta Coding: FoM showing impact of $E_b/N_0$ on video quality for $F_d=10\text{Hz}$ , Beta =50% .....	64
5.7 No perceptual difference observed between Left picture ( $E_b/N_0=33.5\text{dB}$ ) and Right picture ( $E_b/N_0=53\text{dB}$ ).....	64
5.8 Hybrid Beta Coding: Impact of $F_d$ on video quality @ $E_b/N_0$ =53dB and Beta=50% .....	66
5.9 Hybrid Beta Coding: Left picture impacted by $F_d=10\text{Hz}$ and right picture impacted by $F_d=100\text{Hz}$ .....	66
5.10 Hybrid Beta Coding: FoM plot for Beta = 50% and Beta =100%	68
5.11 Comparison: Hybrid Beta Coding (Beta=50%) vs Pure Digital Coding .....	69
5.12 Subjective comparison: Left picture(Hybrid Beta Coding Beta =50% has shades of brightness) vs Right picture (Pure Digital Coding) .....	69
5.13 Comparison: Hybrid Coding by DCT ordering vs Pure Digital Coding .....	71
5.14 Subjective comparison: Left picture(Hybrid Coding by DCT ordering has feeble distortions) vs Right picture (Pure Digital Coding).....	72

## CHAPTER I

### INTRODUCTION

With the latest advancements in wireless communication technology and video compression technology, applications such as video mobile phone and TV on a mobile will become a reality in the near future. Despite, these technology advancements, wireless communication of video and audio signals still faces difficult challenges from wireless fading channels. Strict delay constraints of a video signal make wireless video transmission a more challenging research topic. Hence it is imperative to study the effects of a wireless channel on video transmission. One of the aims of this research is to study the effects of the typically encountered wireless Rayleigh fading channel on a video transmission based on the latest video coding standard. H.264 aka Advanced Video Coding (AVC) is the latest video compression standard jointly developed by the Motion Pictures Experts Group (MPEG) and Video Coding Experts Group (VCEG). The H.264 video coder is designed for both conversational (video telephony) and non conversational video applications (video streaming). This research studies the effects of a Rayleigh fading channel on a compressed H.264 video stream for various bit error rates (BER), signal to noise ratios ( $E_b / N_0$ ) and Doppler rates and evaluates the performance of various source coding features and suggests which is best at which BER,  $E_b / N_0$  and Doppler rates.

In the second part of this research, alternative source coding is considered. This alternative source coding uses a combination of digital and analog coding of video bit streams, hereafter referred to as a hybrid coding scheme for compressed video transmission. Performance of this scheme is studied in presence of a Rayleigh fading

---

This thesis follows the style of *IEEE Transactions on Circuits and Systems for Video Technology*.

channel for various bit error rates (BER), signal to noise ratios ( $E_b/N_0$ ) and Doppler rates. The hybrid scheme is also compared with the pure digital scheme which is being studied in the first part of the research.

Chapters are organized as follows. Chapter II gives some introduction on video coding and specifically the H.264 standard. Chapter III covers some background information on wireless Rayleigh fading channels. Chapter IV explains the first part of the research. Broadly it covers RTP packetization schemes, frame erasure processing, system block diagram and various simulation results with some important conclusions. Chapter V covers the second part of the research. Broadly it explains two hybrid source coding techniques supported with experimental results from simulation. Chapter VI concludes the research work.

## CHAPTER II

### BACKGROUND INFORMATION ON H.264

#### A. Introduction

H.264 aka AVC is the latest video compression standard jointly developed by the Motion Pictures Experts Group (MPEG) and Video Coding Experts Group (VCEG). The standard is currently owned by International Telecommunication Union-Transmission (ITU-T) under the standard Recommendation H.264 and by International Standard Organization (ISO) under the entitled name 14496-10 Advanced Video Coding (AVC). H.264 is otherwise referred to MPEG-4 part10. This new standard is far superior to earlier video coding standards such as H.263 and MPEG-4, in terms of compression efficiency.

The standard is 50% more compression efficient than the earlier standards. This efficiency is not achieved by one single functional unit or block that is 50% more efficient. Instead this efficiency is achieved by improving several functional units or blocks of the standards such as motion compensation, inter prediction, intra prediction, transformation, quantization and more importantly improved context adaptive entropy coding techniques. In the following paragraphs, some video compression basics will be discussed followed by an overview of the H.264 codec (encoder and decoder) and finally concluded with a list of some potential applications of this codec.

#### B. Video Standard Basics

Each picture in a progressive or interlaced video signal is represented by a frame of pixels and in an interlaced video signal as fields. A frame consists of two fields, a Top field and a Bottom field. A Top field captures the odd lines of a frame and a Bottom field captures the even lines of a frame. Each frame/field is encoded by a video encoder

and finally transmitted as a bitstream to a receiver. Each frame in an encoded video bitstream is identified by a frame number and similarly each coded field has an associated picture order count.

The Display order of a video sequence is defined as the order in which a video sequence is played back. The Decoding order of a video sequence is defined as the order in which a video signal is encoded. The display order can be different from the decoding order. The Frame number deals with the display order, whereas the picture order count deals with the decoding order of fields.

The standard supports various Chroma subsampling modes such as 4:2:0, 4:2:2 etc. In 4:2:0 Chroma subsampling, for every 4 Luma samples, there are 2 Chroma (Cb) and 2 Chroma (Cr) samples. From here onwards 4:2:0 Chroma subsampling is assumed unless otherwise specified. A coded picture consists of several MacroBlocks (MB)s. Each MB consists of 16 x 16 luma samples, 8 x 8 Chroma Cb samples and 8 x 8 Chroma Cr samples. For example, in a QCIF (176 x 144 pixels) picture format, a coded picture consist of 99 MacroBlocks. Within a picture, macroblocks are grouped into slices. A slice is composed of several macroblocks arranged in raster scan order but not necessarily in a contiguous manner. These are generally subsets of a given picture which can be decoded independently. There are three types of slices based on the type of prediction applied to macroblocks belonging to that slice. An Intra (I) slice consists of only Intra (I) macroblocks, a Predictive (P) slice may contain both I and P macroblocks and a Bi-predictive (B) slice may contain I and B macroblocks.

If a macroblock is predicted based on neighboring coded macroblocks within a picture it is referred to as intra prediction and if a macroblock is predicted based on neighboring macroblocks of previously coded picture it is referred to as inter prediction. Previously coded pictures are saved and may be used as reference pictures for inter prediction of the current picture and further coded pictures.

An I macroblock is predicted using intra prediction of decoded samples of neighboring macroblocks within a current slice. There are several prediction modes available for intra prediction and a subset of these modes are available for various block



types, depending on whether the prediction is formed from a 16 x 16 Luma block or 4 x 4 Luma block or 8 x 8 Chroma block.

A P macroblock is predicted using inter prediction from reference pictures. Reference pictures are organized into two lists. List 0 is used for predicting P macroblocks. List 1 is used for predicting B macroblocks. Inter prediction is a partition and a sub partition based prediction, where each inter coded macroblock can be divided into several macroblock partitions of block sizes 16 x 16, 16 x 8, 8 x 16, and 8 x 8 Luma and associated Chroma samples. If 16 x 8 partition size is chosen as the best partition, then for the current macroblock total prediction error from using 16 x 8 partition size is the least compared to the other partition sizes. Hence the current macroblock will be predicted using inter prediction of two 16 x 8 blocks. However if in 8 x 8 partition is chosen as the best partition, then each 8 x 8 macroblock can be divided into several sub-macroblock partitions of subblock sizes 8 x 8, 8 x 4, 4 x 8, 4 x 4 Luma and associated Chroma samples. Similarly the best sub macroblock partition is chosen that yields the least prediction error. A B macroblock like a P macroblock is predicted from reference pictures using inter prediction. A B macroblock is predicted from references pictures in list 0 and list 1.

### **C. H.264 Encoder**

H.264 consists of some basic functional units such as prediction, motion compensation, transformation, quantization, and entropy coding. These functional elements are also present in previous standards but the detail of these functional units distinguishes H.264 from earlier standards. In addition to that H.264 incorporates a deblocking filter. A functional block diagram of a H.264 encoder is shown in Fig. 2.1. The Encoder consists of two dataflow paths. The Forward path deals with encoding a frame or field. The Reconstruction path deals with reconstructing a frame to form references for future predictions.

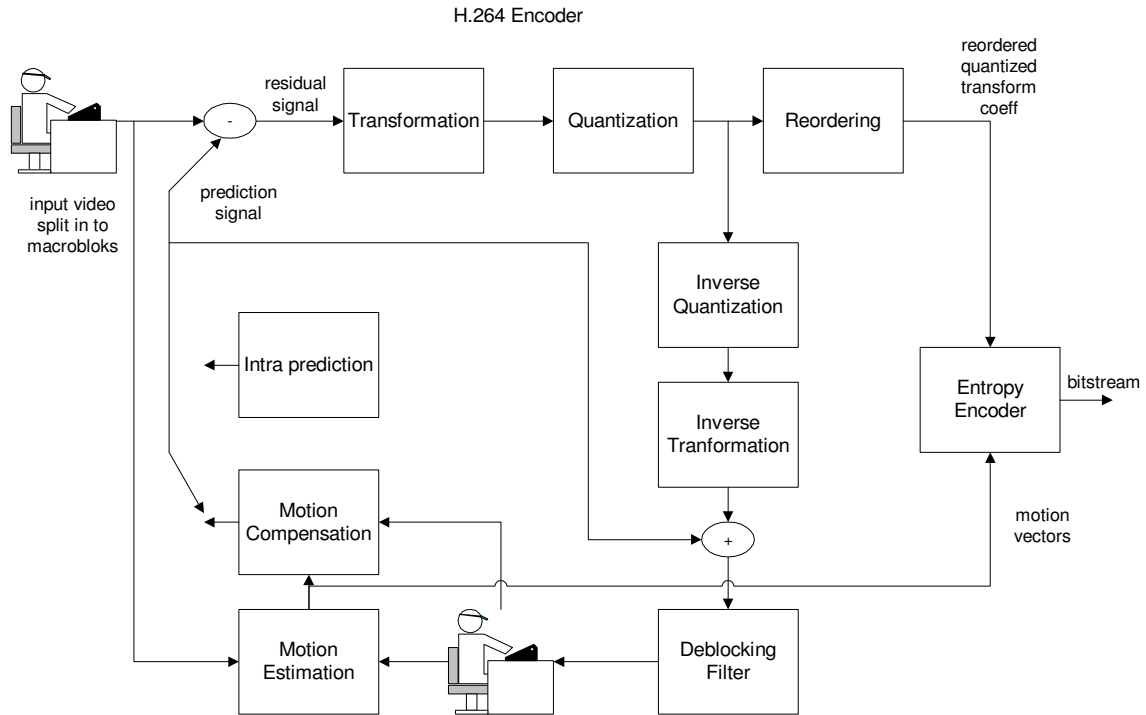


Fig. 2.1. H.264 Encoder block diagram.

The following describes the steps involved in encoding a frame or field within the scope of a macroblock. An input frame is processed in units of macroblocks. A macroblock is intra or inter encoded. Typically all macroblocks in the first frame of a video sequence are intra coded. In intra mode, the prediction signal for the current macroblock is formed from spatially neighboring samples that have been previously encoded in the current slice. The prediction signal is formed based on the chosen prediction mode which yields the least prediction error or residual. Prediction residual is computed by subtracting the prediction signal from the original samples. Macroblocks of subsequent frames of a video sequence are inter coded or intra coded whichever yields least prediction error between the original signal and the predicted signal. Often, macroblocks of remaining frames are inter coded. In inter coding a prediction signal is formed from a reference frame by motion compensation and motion estimation. Motion estimation will determine the motion vector which minimizes the prediction error.

Motion compensation will apply the estimated motion vector displacement to the reference picture to form the prediction signal, which is subtracted from the original samples to yield a prediction error/residual. Motion vectors are encoded and transmitted as side information. But encoding a motion vector of each macroblock partition or sub partition will cost a significant number of bits. In order to save bits, motion vector prediction will predict the motion vector of the current partition or sub partition based on the motion vector information of neighboring partitions or sub partitions. Motion vector difference between the current vector and the predicted vector is encoded and transmitted.

The residual signal is first transformed using DCT transform, and then scaled. The scaled transformed coefficients are quantized and then entropy coded. Sophisticated entropy coding schemes such as Context Adaptive Binary Arithmetic Coding (CABAC) and Context Adaptive Variable Length Coding (CAVLC) are employed. The coded data is transmitted as a bitstream.

The reconstruction path of the encoder is a mini decoder which deals with inverse quantization and inverse transformation of quantized DCT coefficients. Inverse transformed DCT coefficients will form the reconstructed residual signal which is then added to the prediction signal already computed in the forward path of the encoder to form the reconstructed macroblock. The reconstructed macroblock is filtered using a deblocking filter to reduce blocking distortion, by smoothing the block edges thereby improving the appearance of a reconstructed frame. These frames are used as references for further prediction.

#### **D. H.264 Decoder**

H.264 Decoder is very similar to the reconstruction path of H.264 Encoder. Additional components include the depacketizer and entropy decoder. The depacketizer strips the compressed bitstream from the received Network Abstraction Layer (NAL) unit. The Entropy decoder decodes the received bitstream to generate quantized DCT coefficients

and forms a prediction signal based on the received prediction modes and motion vector information. The rest of the procedure is the same as the reconstruction path of the encoder. For more detailed information on H.264, the reader is advised to refer to [1].

### **E. Highlights of H.264**

Here, the subset of the salient features of H.264 that lead to superior compression efficiency that distinguished H.264 from its earlier counterparts are listed. Readers are advised to refer to [1] & [2] for more information.

1. Variable block size motion compensation
2. Multiple reference pictures up to 16 for motion compensation
3. Superior reference buffering scheme
4. weighted prediction
5. Quarter sample accurate motion compensation
6. Small block size transforms
7. Arithmetic coding
8. Context adaptive entropy coding
9. Deblocking filter.

### *Applications*

The following three applications were considered as part of the design of H.264:

1. Conversational applications such as video telephony and video conferencing, which is very delay intolerant. Errors are allowed within tolerable limits, and the limit is purely based on the error concealment techniques implemented in the decoder.
2. Download applications, where pre coded video streams can be downloaded and then played back locally. They are transported through very reliable protocols

such as FTP, TCP. Errors are disallowed in these applications. They do not impose any delay constraints.

3. IP-based video streaming, the delay requirements for this application is somewhere in the middle between download and conversational applications.

These applications can either be transmitted through wireline or wireless. Wireless technologies although being cost effective in implementation, pose serious challenges to real time video transmission applications. The focus of this research is to come up with a metric that defines the SNR (Signal to Noise Ratio) and the BER (Bit Error Rate) that yields acceptable video quality in a subjective sense for various source coding techniques of H.264 for various channel conditions determined by Doppler rate for an uncoded compressed video transmission over a Rayleigh fading channel. As part of this research, hybrid transmission schemes namely, analog and digital transmission of compressed video signals are also considered.

## CHAPTER III

### BACKGROUND INFORMATION ON RAYLEIGH FADING CHANNELS

#### A. Introduction

In this chapter some background information on Rayleigh fading channels and their properties are discussed. Since the focus of this research is to evaluate video transmission quality over Rayleigh fading channels, it is imperative to understand the characteristics of this channel and to understand the wireless channel simulator implementing the same.

The signal received at the receiver is composed of a signal from a line of site path if present plus signals reflected off surfaces, buildings, trees etc. These signals with different attenuations arrive at different times contributing different phase shifts. These phase shifts from different paths can sometime add constructively leading to a stronger signal and at sometimes can add destructively to cancel each other leading to a weaker signal. This process is termed fading.

When the line of site path is not present and there are large numbers of paths of similar magnitude, then the channel can be modeled as a Rayleigh fading channel [3]. A Rayleigh fading channel is typically encountered in land mobile channels, where line of site paths are rare. Received signals in a multipath channel can be modeled as,

$$g_r(t) = \sum_k \rho_k e^{j\theta_k} g_s(t - \tau_k) + N(t) \quad (3.1)$$

Where,

$g_r(t)$  = complex envelope of the received signal

$g_s(t)$  = complex envelope of the transmitted signal

$\rho_k$  = attenuation of the  $k$  th path

$\theta_k$  = phase shift of the  $k$  th path

$\tau_k$  = delay of the  $k$  th path.

If delay spread  $\tau_m$  is defined as the maximum delay difference between two significant paths, then for the case when  $\tau_m$  is almost negligible compared to the symbol period, then the above equation (3.1) becomes

$$g_r(t) = hg_s(t) + N(t) \quad (3.2)$$

Where,

$h = x + jy = ae^{j\phi} = \sum_k \rho_k e^{j\theta_k}$  is a zero mean complex Gaussian random variable defined

by

$$f_{x,y}(x, y) = \frac{1}{2\pi\sigma^2} e^{-\frac{x^2+y^2}{2\sigma^2}} \quad (3.3)$$

Its magnitude  $a$  follows a Rayleigh distribution given by

$$f_a(a) = \frac{a}{\sigma^2} e^{-\frac{a^2}{2\sigma^2}} U(a) \quad (3.4)$$

The phase  $\phi$  follows uniform distribution given by

$$f_\phi(\phi) = \frac{1}{2\pi}, 0 \leq \phi < 2\pi \quad (3.5)$$

## B. Power Spectrum of Rayleigh Fading Process

The power spectrum of land mobile fading channel is defined as

$$PSD(f) = \frac{P_r}{\pi\sqrt{1-(f/f_d)^2}}, f < f_d \quad (3.6)$$

and the corresponding autocorrelation function is

$$R(\tau) = P_r J_0(2\pi f_d \tau) \quad (3.7)$$

where,

$P_r$  = Received power

$f_d$  = maximum Doppler shift

Power Spectral Density (PSD) and the corresponding autocorrelation function of a Rayleigh fading channel are shown in Fig. 3.1 and Fig. 3.2. For more detailed description and derivation of above quantities, readers are advised to refer to [4] & [5].

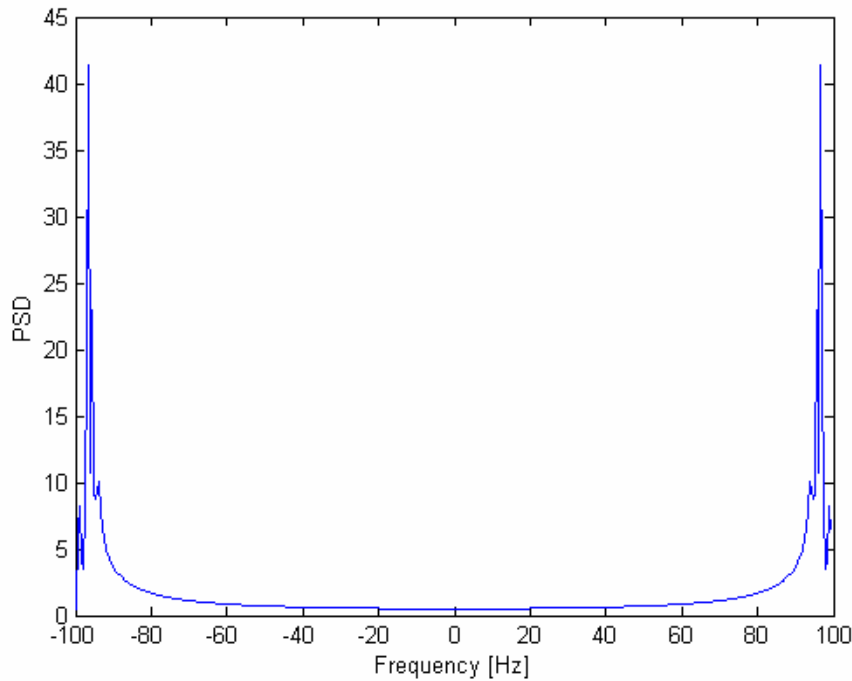


Fig. 3.1. PSD of a Rayleigh fading process. Maximum doppler shift is 100Hz.

### C. Time Domain Method

All experiments in this research are carried out in a computer. In order to get accurate results, It is required to make sure that simulator results are as close as possible to the theoretical results. Since this research is trying to evaluate the video transmission



quality over Rayleigh fading channel, an accurate representation of Rayleigh fading channel in computer is mandatory. Filter based Time Domain method is used for simulating a Rayleigh fading process.

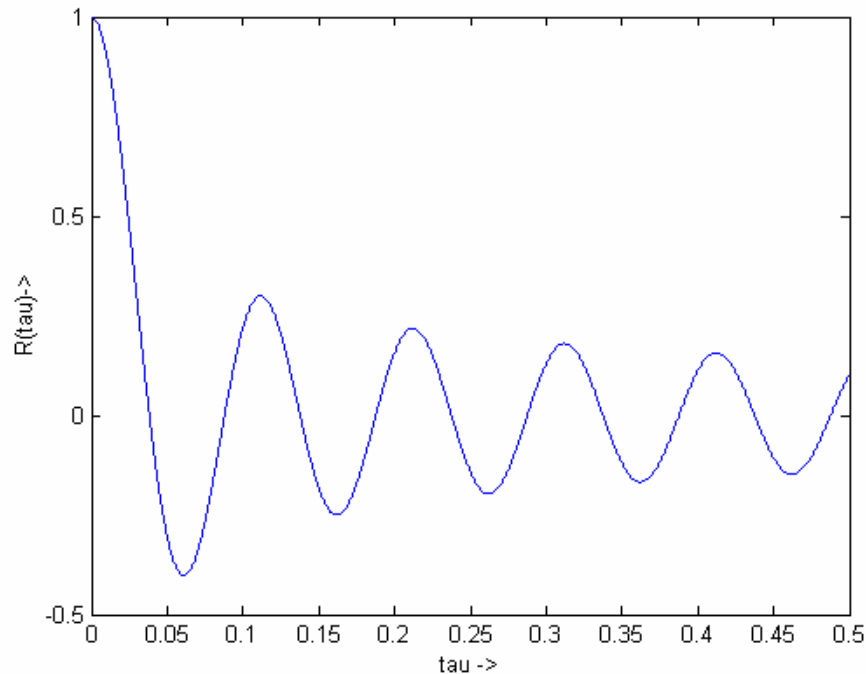


Fig. 3.2. Autocorrelation function of a Rayleigh fading process.

The Time Domain method is a filter based implementation. This method is employed in this research because, simulating very large sequence of a Rayleigh fading process is time and memory consuming. Hence it is necessary to simulate smaller chunks of the Rayleigh fading process in order to aid faster implementation. It is also necessary to prevent discontinuities at the boundaries of the smaller chunks. A brief description of the time domain method is presented below. Readers needing more information please refer to [5] & [6].

In the Time Domain method, a third order filter is designed to generate a realization of a Rayleigh fading process. The input signal consists of a zero mean, unit

variance complex Gaussian random process and is passed through this filter to generate a realization of a Rayleigh fading process. The first few samples (equal to the length of impulse response of the filter) of the output of the filter can be discarded as transients.

The third order filter is implemented as a cascade of first and second order filters. The first order filter is given by

$$H_1(s) = \frac{\omega_0}{s + \omega_0} \quad (3.8)$$

The second order filter is given by

$$H_2(s) = \frac{\omega_0^2}{s^2 + 2\xi\omega_0s + \omega_0^2}$$

$$\omega_0 = \frac{2\pi f_d}{1.2}, \xi = 0.175 \quad (3.9)$$

The magnitude (expressed in dB) and phase component of one realization of a Rayleigh fading process simulated through the time domain method are shown in Fig. 3.3 and Fig. 3.4.

#### D. Important Results

For a given  $E_b / N_0$ , the probability of error of a BPSK (Binary Shift Keying) modulated signal transmitted over a Rayleigh fading channel is given by

$$P_e = \frac{1}{2} \left[ 1 - \sqrt{\frac{E_b / N_0}{1 + E_b / N_0}} \right] \approx \frac{1}{4E_b / N_0} \quad (3.10)$$

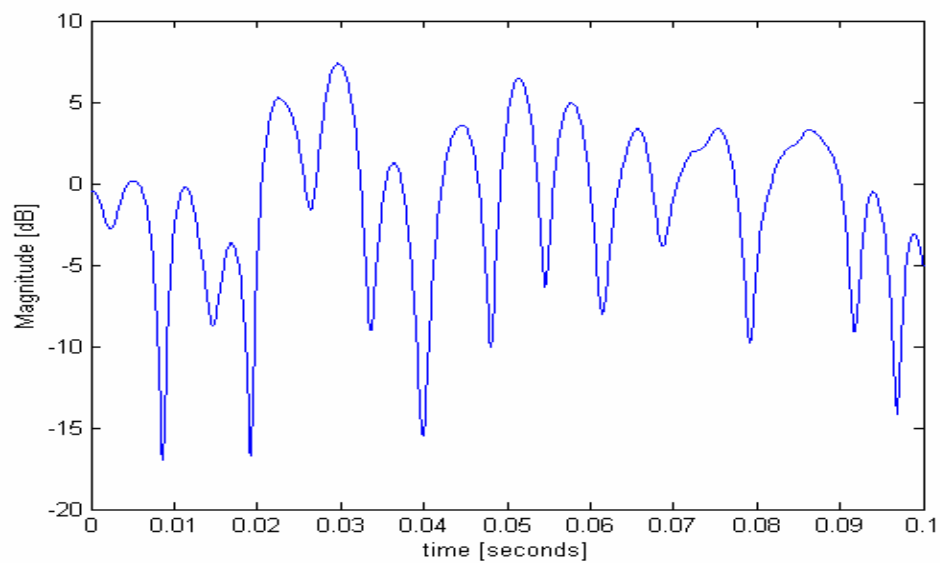


Fig. 3.3. Magnitude response of a Rayleigh fading process.

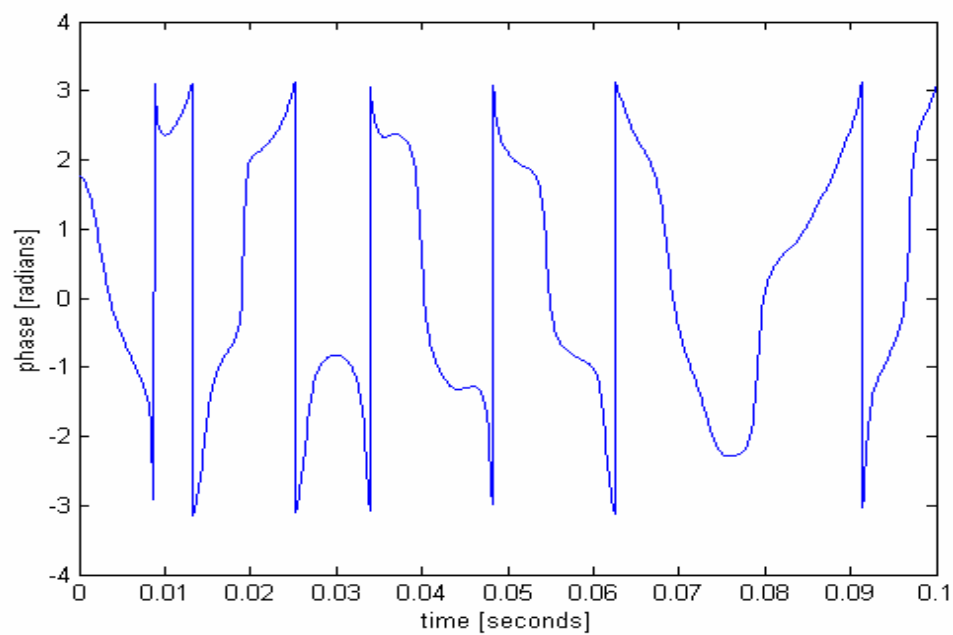


Fig. 3.4. Phase response of Rayleigh fading process.

## CHAPTER IV

### VIDEO TRANSMISSION OVER RAYLEIGH FADING CHANNELS

#### A. Introduction

Wireless fading channels pose some serious challenges to data and real time communication. Nevertheless, wireless communication systems are preferred over wireline communication system, for its lower system cost, lower implementation cost and higher return on investments for carriers. Data communication over wireless channels is not a major concern, since data transmitted are delay tolerant, and need only to be reliable. This can be achieved by reliable transmission protocols such as TCP/IP (Transmission Control Protocol/ Internet Protocol). However real time communication of video signals mandate strict delay constraints, though 100% reliability need not be guaranteed. Errors are allowed within some tolerable limits in real time communication of video signals. Hence there is significant research going on in parallel in two research communities, the communication community and the multimedia community. The communication research community is aimed at providing advanced coding and modulation techniques to take care of the errors introduced by fading and noise. The multimedia research community is aimed at providing advanced source coding techniques to satisfy strict bandwidth requirements and delay constraints of wireless fading channels. The outcome of their research led to the H.264 video coding standard.

One of the main focuses of this research is to evaluate this compressed video quality in wireless channel environments. There are papers and publications available in the literature [7] & [8] that have looked at this problem in a network engineering perspective. Chapter I briefly discusses three intended applications for a video coder. Video download application is a non real time application calling for reliable transport mechanism using TCP/IP. It is mentioned by the Stephen Wenger in [8] that “ Most of the traditional video coding research somewhat implies this type of application”. Other

literature that is relevant to this research are mentioned below. A review of H.264 in wireless environments is provided by T.Stockhammer et al.[9]. S.Zhao, Z.Xiong and X.Wang [10] looked at providing efficient joint source channel coding scheme for wireless video over CDMA networks. Similarly [11] to [17] also discusses providing a robust channel coding scheme for wireless video over CDMA networks. In the recent past, error concealment schemes for wireless video applications are dealt with by many researchers. A comprehensive review of error concealment schemes is available at [18]. The papers [19] to [22] deals with error concealment in packet based video transmission. Most of the research is centered on evaluating video transmission quality in a packet erasure wireless channel. Authors of [23] to [26] looked at the problem of transporting video over a packet erasure and fading channels. Their focus is on packet losses and bit errors resulting from packet losses. For example if a packet of size 100 bytes is received erroneously because few bytes in that packet are corrupted, the decoder will discard the whole packet and all 800 bits are erased, whereas only a few bits actually got flipped by the wireless physical channel. This research looks at the problem more from a communication engineering perspective i.e. more at a physical layer level. The research deals with the most commonly encountered wireless channel, the Rayleigh fading channel and study the effects of the Rayleigh fading channel on a compressed video stream for various bit error rates (BER), signal to noise ratios ( $E_b / N_0$ ) and Doppler rates and suggest which source coding scheme is best at which BER,  $E_b / N_0$  and Doppler rates.

The remainder of this chapter is organized as follows, section B discusses the system setup and the functional units involved in the system briefly. Section C discusses a modified version of RTP packetization scheme in more detail. Section D describes the error concealment techniques that have been used in addition to the techniques that are already part of the H.264 implementation. Finally the chapter concludes with experimental results and some important conclusions in section E.

## B. System Setup

The functional block diagram of the wireless communication system under test is shown below in Fig. 4.1 and Fig. 4.2. A video signal is fed as input to an H.264 encoder. The H.264 encoder can accept various video signal formats, but only the QCIF format which is 176 (width) x 144 (height) pixels video frame is considered here. The encoded video bit stream is fed to the RTP (Real time Transport Protocol) packetizer, which churns out fixed length RTP packets embedded with CRC bits for error detection at the receiver end. The packet bitstream is BPSK modulated and sent over the wireless channel. The transmitted symbols interact with the environment in a complex way affecting the video quality at the receiver. Interaction with the environment is modeled using a Rayleigh fading channel. The Time Domain (filter based) method is used to simulate the Rayleigh fading channel in MATLAB. For a given  $E_b / N_0$  and Doppler frequency, this module generates a realization of a Rayleigh fading process. The BER and  $E_b / N_0$  are related by equation (3.10) in chapter III.

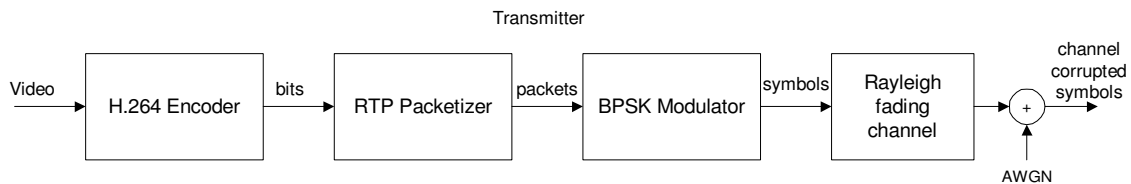


Fig. 4.1. Wireless system setup, Transmitter.

At the receiver, the received packet is verified for any errors by comparing the received CRC bits with the locally computed CRC bits at the receiver. Corrupted packets are sent for error concealment and error free packets are sent for normal decoding. Finally the decoder outputs the video. The above functional units are discussed in more detail in the following sections.

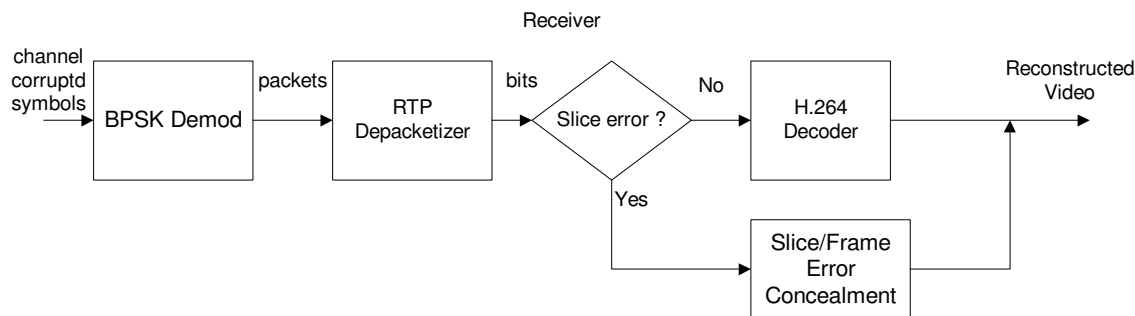


Fig. 4.2. Wireless system setup, Receiver.

### C. RTP Packetization

Before the RTP packetization scheme can be discussed, it is necessary to understand the network interface architecture of H.264. Unlike earlier video coding standards where compressed video is just transmitted as a bit stream, H.264 uses an interface layer to interact with lower layers such as RTP. This Network Abstraction Layer (NAL) is part of the standard and it interfaces the Video Coding Layer ((VCL ) compressed video bit stream) from other lower layers such as RTP. NAL abstracts VCL data from the network related parameters. Hence the VCL data can be transported in a variety of networks such as IP networks, circuit switched networks etc. This network friendliness nature of H.264 is exploited here to transport the NAL packets through RTP. The packet layers of the H.264 encoder are shown below in the Fig. 4.3.

The NAL is used to transmit both VCL data and Non VCL data. VCL data represents the compressed video bit stream, such as encoded motion vectors, encoded quantized DCT coefficients etc. Non VCL data are Sequence Parameter Sets (SPS) and Picture Parameter Sets (PPS). These parameter sets carry very critical information. Without knowing these parameter sets, the decoder does not know how to decode a bitstream. The SPS contains all the information related to a video sequence defined between any two Intra Decoder Refresh (IDR) frames. The PPS contains all the information common to all slices in a single picture.

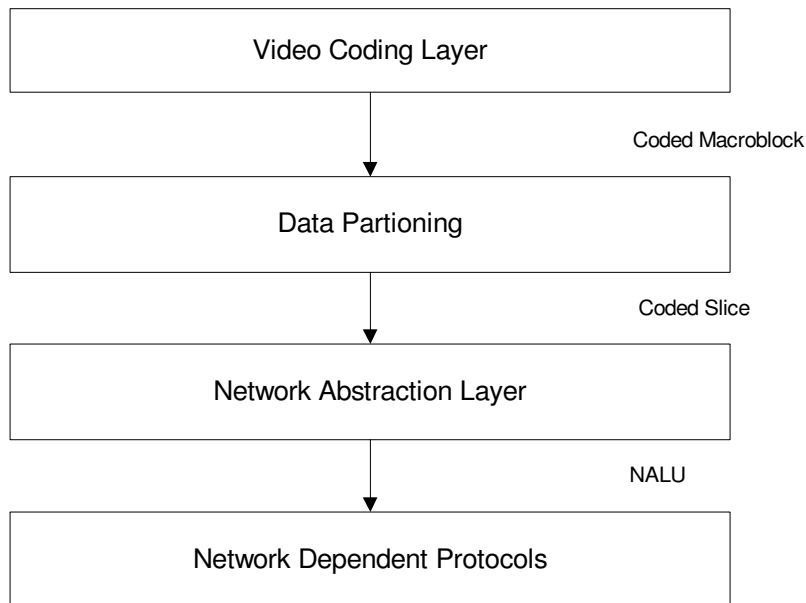


Fig. 4.3. H.264 Encoder packet layers.

Whether it is VCL data or Non VCL data, it is encapsulated into the NAL Unit (NALU). The packet structure of a NALU is shown below in the Fig. 4.4 and a description of the fields is listed in the Table 4.1. The NALU consists of an NALU Header and an NALU payload. For VCL data, the NALU payload carries one slice of information. For Non VCL data, the PPS and the SPS are transmitted in separate NALUs.

F(0)	NRI(1:2)	Type(3:7)	NALU Payload
------	----------	-----------	--------------

Fig. 4.4. NALU packet structure.



Table 4.1  
NALU Packet Structure Field Description

Field	Description	Values
F	Forbidden bit	0, no errors 1, syntax error
NRI	NALU Reference Indicator	00, not used for reference 01, low priority 10, high priority 11, highest priority
Type	NALU defined types	1-31. 28 is used here
NALU Payload	Variable length NALU payload	

For a detailed description of NALU packet structure, please refer to [27].

A simplified RTP packetization scheme is implemented. The RTP packet structure discussed here is a modified version of RFC 3984 [27] and is shown below in the Fig. 4.5. A 32 bit CRC is added to the RTP header. Instead of implementing a data link layer to detect errors, the error detection capability is shifted to the RTP layer and hence the data link layer need not be implemented. This modification is done to keep the complexity of the system under test low and simulation easy. A point to point link between the transmitter and the receiver separated by a wireless channel is assumed. Since the focus of this research is on conversational video applications, due to its very low delay constraints and real time requirements, no retransmission of RTP packets are allowed. Since a dedicated link is assumed, any transport/network (TCP/IP) or data link layer protocol for bandwidth sharing is not implemented. Since emphasis of this research is on the physical layer, bit strings from RTP packets are directly modulated using BPSK modulation and then transmitted over a wireless channel. A fixed length RTP packet is assumed. The NALU is encapsulated into the RTP packet, in other words the RTP payload carries NALU.

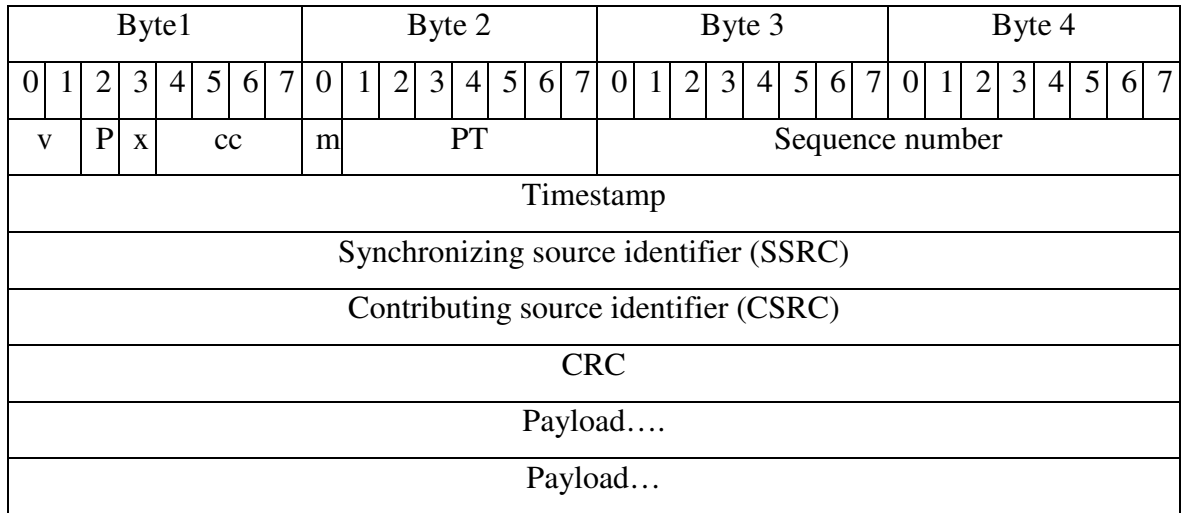


Fig. 4.5. RTP packet structure for H.264.

Among all the fields, the fields that are relevant to this research are shown below in the Table 4.2. For readers interested in more details, please refer to [27] & [28]

Table 4.2  
RTP Packet Header Field Description for H.264

Field	Description	Value
M	Marker bit	1, for the last RTP packet in a coded picture 0, otherwise
PT	Payload type for H.264	105
Sequence number	To determine the decoding order of NALU	16 bits
Time stamp	Sampling time instant of a picture	32 bits
CRC	Cyclic redundancy check	32bits

Since the NALU size can be varying and the RTP size is fixed, there is a need to fragment the NALU into several RTP packets. If the NALU size is less than the RTP Payload size, then one complete NALU can be transmitted in a single RTP packet with

the remaining bits padded with zero bits. If the NALU size is greater than the RTP payload size, then the NALU is fragmented into an equal length RTP payload size and the fragmented NALU is encapsulated into an RTP packet. Typically zero bits are padded into the last fragmented NALU to create a fixed length RTP packet. In the RTP literature, this is referred to as fragmented mode. This mandates some changes in the NALU packet structure. The RTP packet structure for transporting partial NALU per RTP packet is shown in Fig. 4.6. Table 4.3 describes the fields involved in the packet.

RTP Hdr	FU indicator			FU Header				FU length	FU payload
	f	nri	Type	S	E	R	Type		
FU payload								Padding	

Fig. 4.6. RTP packet structure for transporting fragmented NALU.

Table 4.3  
Field Description for RTP Packet Structure for Transporting Fragmented NALU

Field	Sub field	Description	Values
RTPHdr		RTP header	20 bytes
Fragmentation Unit (FU) Indicator	F	Forbidden bit	0, no errors (default) 1, syntax error
	NRI	NALU Reference Indicator	00, not used for reference 01, low priority 10, high priority 11, highest priority
	Type	NALU defined types	28
FU Header	s	Start bit	1- first RTP packet of NALU 0- Not the first RTP packet of NALU
	e	End bit	1- Last RTP packet of NALU 0- Not the last RTP packet of NALU

	r	Reserved	0
	Type	NALU defined type	1-23
FU length		Payload length	16 bits
FU Payload		VCL bits	Variable
Padding		Zero bits padding	

The received packet is checked for errors by computing the CRC checksum and verifying it with the received checksum. If a packet is found to be an error, the F bit (Forbidden bit) is set and sent to the error concealment module. Frame erasure processing is discussed in more details in the next section.

#### **D. Frame Erasure Processing**

Frame Error Processing in H.264 consists of *Error Detection* and *Error Concealment Techniques*. Each will be discussed in detail below.

##### *Error Detection*

Errors are detected using Cyclic Redundancy Check (CRC). Each NALU (Network Abstraction Layer Unit) consist of one slice of information. A NALU packet may be fragmented into multiple small RTP packets and are sent over the communication channel. Each fragmented RTP packet is protected with a 32 bit CRC mechanism. The generator polynomial is

$$g(x) = X^{32} + X^{26} + X^{23} + X^{22} + X^{16} + X^{12} + X^{11} + X^{10} + X^8 + X^7 + X^5 + X^4 + X^2 + X^1 + 1 \quad (4.1)$$

A 32 bit CRC is computed in the transmitter side and sent along with the rest of the packet. In the receiver side, the CRC is recomputed from the received packet bit stream. If the recomputed CRC matches the received CRC checksum, then the packet is diagnosed as error free, otherwise the received packet is marked as an error packet. The

Slice belonging to that packet is also marked as an error slice. The following paragraphs discuss the techniques used to conceal the above detected errors.

### *Error Concealment Techniques (ECT)*

Error Concealment is an important section of the video decoder processing. As errors are unavoidable in a transmission medium, there are coding techniques that can keep errors to tolerable limits. Nevertheless, the video decoder must be robust in handling errors to improve the video quality. The ECT technique that will be discussed below can handle errors as low as 1 in 10 bits. The ECT that will be discussed below can conceal errors for the following source coding scenarios.

1. When the picture is encoded as IPPPPPP... i.e. one IDR frame followed by only P frames. This is indicated by IDR PERIOD =0. The ECT does not support errors in B frames.
2. When the picture is encoded using multiple IDR frames. For example IPPPIPP... This is indicated by a non zero IDR PERIOD. In the example above, the IDR PERIOD is set to 3.
3. When the picture is encoded using a single slice per picture. All 99 MacroBlocks (MBs) are encoded in a single slice.
4. When the picture is encoded using multiple slices per picture. For example, 6 macroblocks per slice, 17 slices per picture.

The ECT module consists of the following functional units

1. Slice Parameter Estimation
2. NALU Error Processing
3. Slice Error Processing
4. Reference Buffer Management
5. Intra frame error concealment

## 6. Inter frame error concealment

Slice Parameter Estimation will estimate important slice parameters such as number of slices per picture and number of MBs per slice from an error free slice. NALU error processing will conceal NALU header errors while Slice Error Processing will conceal slice header errors. Reference Buffer Management will manage Decoder Picture Buffer and reference picture list 0 and list 1 in the presence of errors. The corrupted slices are discarded and hence not decoded, but from Slice error processing unit, information regarding which MBs are corrupted will be used to update the buffer pointer (implementation specific). This information is also supplied as input either to the Intra frame error concealment unit or the Inter frame error concealment unit, depending on whether the corrupted frame belongs to an Intra or Inter frame respectively.

### **Slice Parameter Estimation**

One Important functional unit of this ECT is the slice parameter estimation. Given a good (error free slice), the following information is computed only once.

Number of MBs/ Slice (No\_MB\_Per\_Slice)

Number of Slices/Picture (No\_SL\_Per\_Pic)

IDR PERIOD ( IDR\_Prd)

Current Slice Number within a picture or a frame. (Curr\_SL\_No)

This unit expects an error free slice. An error free slice should always follow the picture parameter set and sequence parameter set for this scheme to operate correctly. The Picture parameter set, sequence parameter set and this first slice are assumed error free. This is a very valid assumption, because a corrupted sequence parameter set or picture parameter set will result in the entire video sequence being useless. Similarly, it is very valid to assume that the first slice is error free in order to ensure proper operation

of ECT. This can be achieved by incorporating a robust coding scheme, or by sending redundant parameter sets or slices. The Curr\_SL\_No will range from 0 to No\_SL\_Per\_Pic -1.

### **NALU Error Processing**

The NALU carries one slice of information. This unit conceals errors in the NALU header. NRI is one of the most vital field information carried by the NALU packet. This field will indicate whether the current slice is an IDR slice or a P slice. If this information is corrupted, then the slice will be decoded with wrong information. So it is very important to conceal this parameter.

In the presence of errors, it is imperative to determine whether the current slice belongs to an IDR picture or not. If the first slice of a picture is detected as an error slice, then the current slice is decoded as not an IDR slice. If any other slices of a picture are detected as an error slice, then the previous slice information is used for the current slice. For example if the previous slice belongs to an IDR frame, and if the current slice is received erroneously, then the current slice will be decoded as an IDR slice. Previous slice information is updated after decoding the current slice.

### **SLICE Header Error Processing**

Start MB number Estimation and Concealment: The Start MB number of the current slice is internally estimated and is compared with the start MB number obtained from the received slice header. If a mismatch is detected, the estimated MB number is used as the current start MB number of the slice.

Estimated Start MB number = No\_MBs\_Per\_Slice \* Curr\_SL\_No

### *Picture and Sequence Parameter ID Concealment*

Default picture and sequence parameter set ID is zero. Picture and Sequence parameter set are identified from their index number. At any time during transmission, the encoder can signal different picture parameter or sequence parameter set ID, and this information is signaled in every slice being transmitted. In case of slice errors, the default picture parameter set ID and sequence parameter sequence ID can be used. Also in case of slice errors, the current slice is always decoded as P\_SLICE.

### *Frame Number Estimation and Concealment*

The frame number is decoded from each slice header. The frame number represents the **decoding** order of frames and need not necessarily be the **displaying** order. Frame number is reset to zero at every IDR frame. Hence frame number estimation is based on the IDR period.

If a slice error is encountered and if IDR period is equal to zero (i.e. IPPPPP...) and if it is the first slice in the picture, then the current frame number is computed as the previous frame number plus one. The rest of the slices within the same picture carries the same frame number. For a non-zero IDR period, the frame number is computed modulo the IDR Period.

### *Picture Order Count (POC) Estimation and Concealment*

POC determines the **display** order of the decoded frames, and it is expressed in terms of fields. Each frame can be decomposed into two fields, the Top Field and the Bottom field. The POC is incremented by two for every completed frame. The POC needs to be concealed in case of slice errors. In case of slice errors, for a zero IDR period, POC is incremented by 2 for every complete picture. For non zero IDR period, the POC is a function of the frame number and it is computed as twice the current frame number.



### *New Picture Detection & Concealment*

Decoding of a new picture is detected by comparing the previous slice parameters with current slice parameters. In order to prevent slice errors forcing wrong detection of a new picture, thereby resulting in loss of synchronization between the encoder and the decoder, picture boundaries have to be detected accurately and in case errors, must be concealed. The value of Curr\_SL\_No shall indicate whether it is the first slice of a new picture or a new slice of the same picture. If the first slice of a picture is detected, this indicates the beginning of a new picture otherwise the current slice belongs to the same picture that the previous slice also belongs to. A deblocking filter is disabled in the presence of slice errors.

### **Reference Decoded Picture Buffer Management**

Each frame is encoded and reconstructed at the encoder and stored in a Decoded Picture Buffer (DPB). These frames are identified as either short term reference frame, or long term reference frame or output display frame or not a reference frame. The reference frames for P Slice prediction is stored in the list0. Hence list0 will have short term reference frames and long term reference frames. Short term reference frames are immediately used for prediction, whereas long term reference frames are older pictures kept for a long time in the buffer so that it may be used for inter prediction of later frames. Short term reference frames are identified by their frame number and long term reference frames are identified by a LongTermPicNum. Short term reference frames and long term reference frames are managed by sliding window memory control. Short reference frames in list 0 are ordered in decreasing order of frame number, whereas long term reference frames are ordered in increasing order of LongTermPicNum. If the sum of a short term and long term reference frame equals the maximum number of reference frames, then the oldest short term reference frame is removed from the list. Long term pictures stay in the DPB until explicitly removed. This buffer will be maintained both at

the encoder and decoder. Hence there is a need to conceal this buffer at the decoder in case of slice errors, as slice errors can destroy the synchronization between the encoder and decoder thereby resulting in very poor video quality.

Slice errors can result in choosing a wrong reference frame number in reconstructing the video at the decoder, leading to loss of synchronization at the decoder. This will affect future frame decoding also. In order to prevent this, any error slices or frames must be concealed and the concealed frame must also reside in the DPB. The concealed frames are managed by the sliding window memory control if the frame is identified to be a reference frame. This avoids spreading errors and helps maintain synchronization at the decoder.

### **Intra Frame Error Concealment**

Intra frame error concealment is already part of the H.264 standard. It is included here only for completeness sake and will be briefly discussed. More details about Intra frame error concealment are available in [29] & [30].

Intra frame error concealment is based on Weighted pixel value averaging. In case of slice errors, MBs gets corrupted or lost. Pixels of lost MBs are recovered from the pixels of neighboring correctly received MBs or concealed MBs in a weighted average sense. Each pixel value in the lost MB is concealed by forming a weighted sum of closest boundary pixels of the spatially adjacent MBs. Weights are chosen according to the inverse distance between the pixel to be concealed and the boundary pixel.

## **Inter Frame Error Concealment**

Inter frame error concealment is also already part of the H.264 standard. It is included here only for completeness sake and will be briefly discussed. More details about Inter frame error concealment are available in [31]. A boundary matching based motion vector recovery algorithm for inter picture is implemented in the standard.

In case of slice errors, the motion vector information is also lost. A motion vector recovery algorithm monitors the motion activity in the correctly received slices. If the average length of a motion vector component is smaller than a pre defined threshold, typically a quarter pixel away, indicating that this current frame has not moved even a quarter pixel away, then it is just enough to copy all lost slices from the collocated positions in the reference frame. If the average length of a motion vector component is above the threshold, then motion vectors of the corrupted MBs are concealed based on the neighboring correctly received MB or concealed MB motion vector information. In this case, MBs are concealed one column at a time by scanning the image MB- column wise from left to right edges to the center of the image. In each MB column, consecutive lost MBs are identified and concealed starting from the top and the bottom of the lost area and eventually moving toward to the center of the lost area. As mentioned before, readers interested in more details can refer to [31]. Theories behind the first part of this research are discussed so far. The experimental results of the vast simulations are discussed in the next section.

## E. Experimental Results

RTP packetization, CRC computation, and frame erasure concealment are implemented in the H.264 video codec (JM9.8 software version [32]). A Rayleigh fading channel based on the time domain method is simulated in MATLAB. Physical layer modulation and demodulation is done in MATLAB. Table 4.4 lists some common test conditions that are used in all the simulations/experiments. Table 4.5 lists test conditions that can vary between different experiments

Table 4.4  
Common Test Conditions

Video Sequence	Carphone	Reference Frames	5
Frame Rate	30 fps	RD Optimization	Off
Image Format	QCIF	Frames Encoded	30
Hadamard	On	YUV Sampling	4:2:0
MV Resolution	¼ pel	Symbol Mode	UVLC
B Frames	No	Channel	Rayleigh Fading
Modulation	BPSK		

Table 4.5  
Variable Test Conditions

Macroblocks/Slice	6 or 99	IDR period	0 or 10
$E_b / N_0$ [dB]	24,27,33.5,37.5, 44.5,47.5,53	Doppler [Hz]	10, 50 or 100

In addition to subjectively evaluating the received video quality, it is also necessary to come up with an objective measure. A Figure of Merit ( $FoM$ ) is computed as

$$FoM = 10 * \log_{10} \left( \frac{e_{ref\_x}}{e_{ref\_x} + e_{diff\_x}} \right)$$

$$e_{ref\_x} = \sum_{w=0}^W \sum_{h=0}^H (x_{ref}[w][h])^2$$

$$e_{diff\_x} = \sum_{w=0}^W \sum_{h=0}^H (x_{ref}[w][h] - x[w][h])^2$$
(4.2)

Where  $e_{ref\_x}$  is the energy of the reference frame which is generated in the reconstruction path of the encoder. In error free conditions, the decoder must produce bit precise representation of this reference frame. In such error free conditions  $e_{diff\_x}$  is zero and hence  $FoM$  is equal to 0 dB. In case of errors,  $e_{diff\_x}$  will be a non zero value and hence  $FoM$  will result in negative dB. Hence  $FoM$  indicates the deviation of the decoded frame from the reference frame.  $FoM$  can be computed for Luma (Y), or Chroma coefficients. For Luma,  $(W, H) = (176, 144)$  and for Chroma  $(W, H) = (88, 72)$ . The  $FoM$  measure is used extensively in this chapter and the following chapter. It is assumed that  $FoM$  is computed only for Luma coefficients unless otherwise stated.

The BER for a BPSK modulated Rayleigh fading channel for various  $E_b / N_0$  against different Doppler frequencies are listed below in the Table 4.6. It is evident that the BER is independent of  $Fd$ , which agrees with the theory. Experimental results are discussed below in the rest of this chapter.

Table 4.6  
 $E_b / N_0$  - BER Relationship for Various  $Fd$

	Bit Error Rate (BER) for various Doppler Frequency( $Fd$ )		
$E_b / N_0$ [dB]	10Hz	50Hz	100Hz
24	$10^{-3}$	$10^{-3}$	$10^{-3}$
33.5	$1.1740 * 10^{-4}$	$8.9779 * 10^{-5}$	$1.0359 * 10^{-4}$
37.5	$5.7551 * 10^{-5}$	$4.6041 * 10^{-5}$	$2.5322 * 10^{-5}$

Table 4.6 continued

$E_b / N_0$ [dB]	Bit Error Rate (BER) for various Doppler Frequency( $Fd$ )		
	10Hz	50Hz	100Hz
44.5	$6.9061 * 10^{-6}$	$1.1510 * 10^{-5}$	$9.2081 * 10^{-6}$
53	$2.1909 * 10^{-6}$	$2.2519 * 10^{-6}$	$2.3020 * 10^{-6}$

### Experiment 1

In this experiment the effect of  $E_b / N_0$  on received video quality is highlighted. The test conditions for this experiment are listed below in the Table 4.7.

Table 4.7  
Experiment 1 Test Conditions

Macroblocks/Slice	6	IDR period	0
$E_b / N_0$ [dB]	24,27,33.5,37.5, 44.5,47.5,53	Doppler [Hz]	10

$FoM$  is plotted for different  $E_b / N_0$  in Fig. 4.7. It is observed subjectively that video quality is good at  $E_b / N_0 = 37.5$ dB and there are no perceptual differences with respect to those with  $E_b / N_0 > 37.5$ dB. This is clearly evident from the Fig. 4.7 where the  $FoM$  curve for 37.5dB is very close to the 0dB line. Shown in Fig. 4.8 is frame 1 from the Carphone sequence. Distortions are clearly seen in the left picture (24dB) and whereas these distortions are absent in the right picture (37.5dB). It can be concluded from this experiment that for an uncoded wireless system, it is enough to transmit a video signal with  $E_b / N_0 = 37.5$ dB with good quality video reconstruction at the decoder. An  $E_b / N_0$  of 37.5dB corresponds to a  $BER = 5 * 10^{-5}$ .

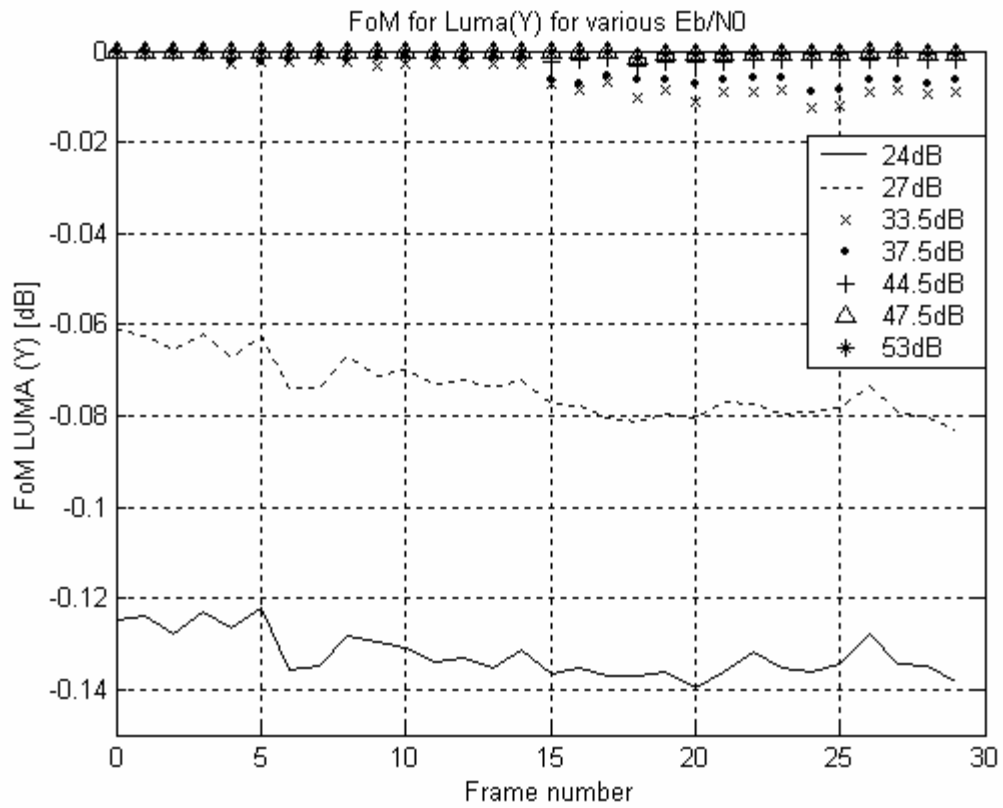


Fig. 4.7. FoM @  $F_d=10\text{Hz}$ , IDR Period=0, 6 MBs/slice for various  $E_b/N_0=24\text{dB}$  to  $53\text{dB}$ .

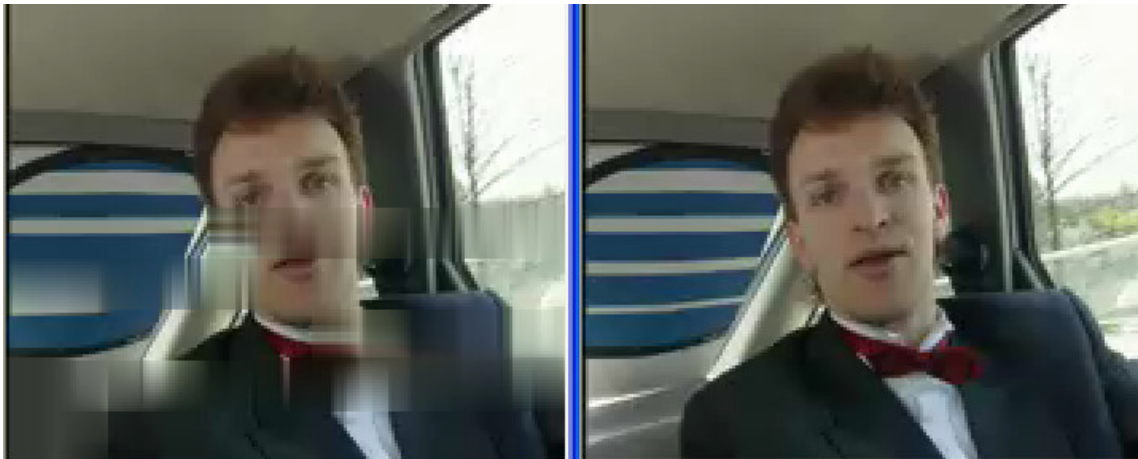


Fig. 4.8. Frame 1: Distortion observed in left picture ( $E_b/N_0=24\text{dB}$ ). Right picture ( $E_b/N_0=53\text{dB}$ ) is distortion free.

By using advanced channel coding techniques and diversity techniques,  $E_b / N_0$  can be reduced significantly maintaining the same BER. It can also be concluded that  $BER=5 * 10^{-5}$  is sufficient to transmit a video signal over a Rayleigh fading channel.

### *Experiment2*

In this experiment the effect of Doppler frequencies on video transmission is explored. The Test condition for this experiment is listed below in the Table 4.8.

Table 4.8  
Experiment 2 Test Conditions

Macroblocks/Slice	6	IDR period	0
$E_b / N_0$ [dB]	37.5	Doppler [Hz]	10,50,100

It can be clearly seen from Fig. 4.9 and Fig. 4.10, that there is significant distortion observed at the 100Hz Doppler frequency. There are no performance differences observed at either 50Hz or 10Hz Doppler frequencies. Hence it can be concluded that the video transmission is tolerant up to 50Hz Doppler frequency.



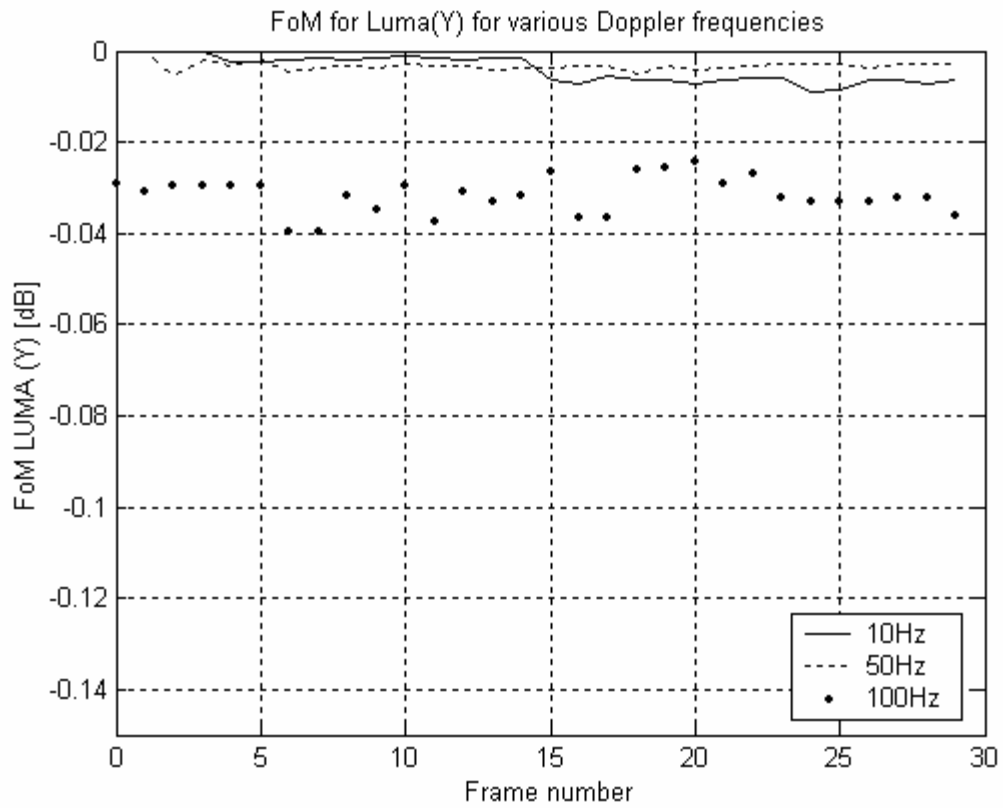


Fig. 4.9. FoM @  $E_b/N_0=37.5\text{dB}$ , IDR Period=0, 6 MBs/slice for  $F_d = 10\text{Hz}, 50\text{Hz}, 100\text{Hz}$ .

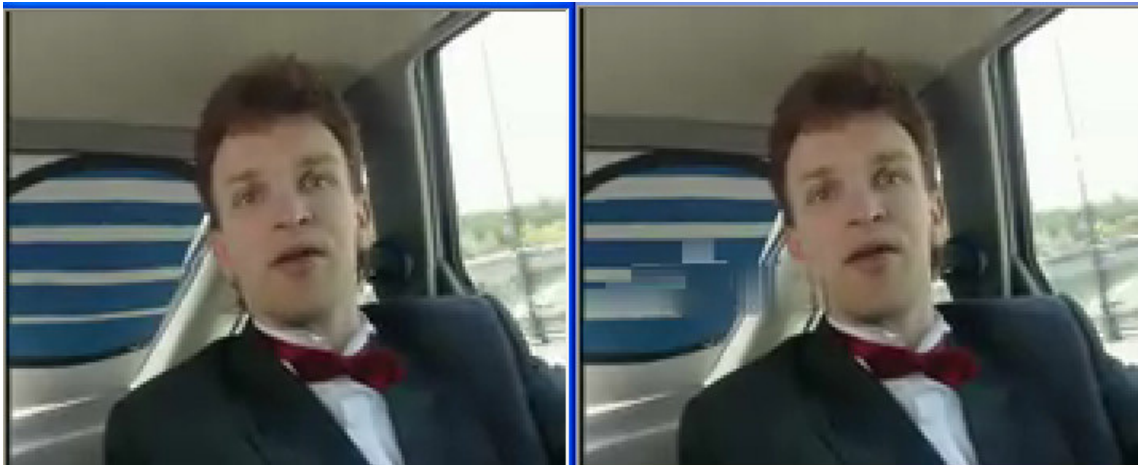


Fig. 4.10. Frame 1. Left picture ( $F_d=50\text{Hz}$ ) is distortion free. Right picture ( $F_d=100\text{Hz}$ ) has distortions.

### Experiment 3

In this experiment  $FoM$  is plotted for various  $E_b/N_0$  and Doppler frequencies to deduce the minimum  $E_b/N_0$  and maximum tolerant Doppler frequency for video transmission over Rayleigh fading channel. Test conditions for this experiment are listed in the Table 4.9.

Table 4.9  
Experiment 3 Test Conditions

Macroblocks/Slice	6	IDR period	0
$E_b/N_0$ [dB]	37.5, 44.5	Doppler [Hz]	10,50,100

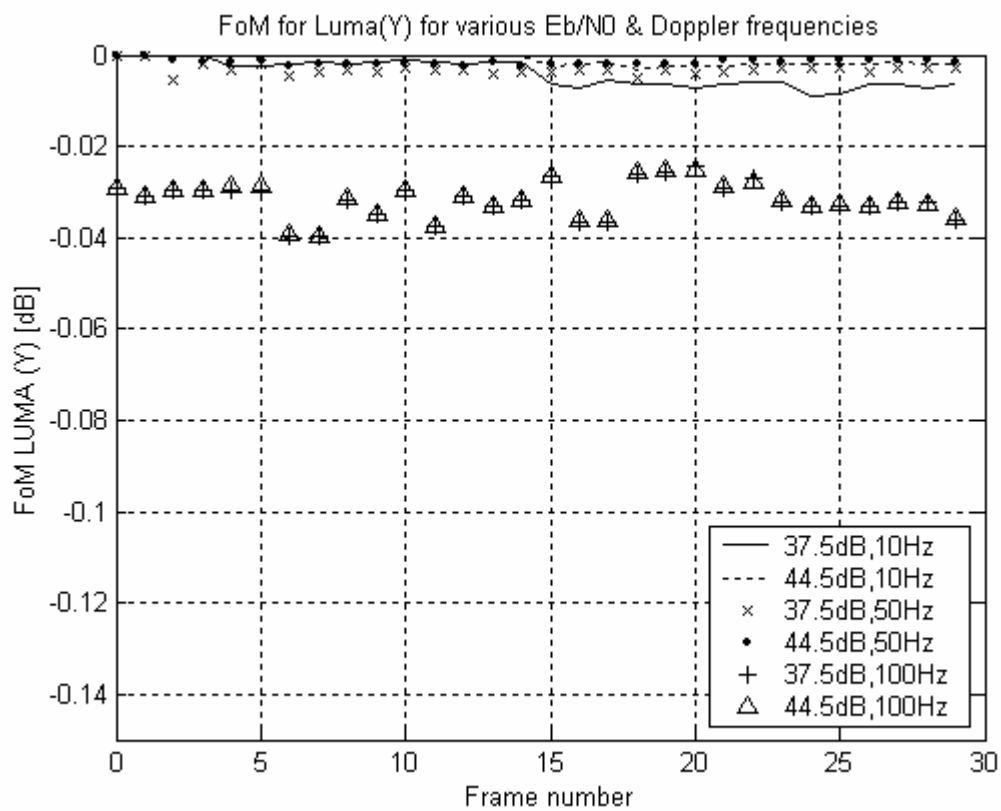


Fig. 4.11. FoM @  $E_b/N_0=37.5\text{dB}, 44.5\text{dB}$ , IDR Period=0, 6 MBs/slice for  $F_d = 10\text{Hz}, 50\text{Hz}, 100\text{Hz}$ .

It can be seen from Fig. 4.11, that performance at 37.5dB, 50Hz Doppler is equivalent to 44.5dB, 50Hz Doppler, 37.5dB,10Hz Doppler and at 44.5dB,10Hz Doppler. Hence it can be concluded that it is sufficient for a video signal coded at 6MBs/slice, and IDR period equal to zero, to be transmitted by an uncoded wireless system with  $E_b / N_0 = 37.5\text{dB}$  over time varying Rayleigh fading channel contributed by 50Hz Doppler frequency. This again agrees with the results of experiment 1 and experiment 2.

#### *Experiment 4*

Test conditions for this experiment are listed in the Table 4.10. This is similar to experiment 3, except for the IDR period is set to 10. Here an IDR frame repeats every 10 frames. Non zero valued IDR period also means higher data rates. From subjective evaluations of the received video, it can be deduced that it is enough to transmit a video signal over a Rayleigh fading channel with  $E_b / N_0 = 47.5\text{dB}$  at Doppler frequency =50Hz. This can also be verified in the Fig. 4.12 where  $FoM$  is plotted for various  $E_b / N_0$  and Doppler frequencies.

Table 4.10  
Experiment 4 Test Conditions

Macroblocks/Slice	6	IDR period	10
$E_b / N_0$ [dB]	24,27,33.5,37.5, 44.5,47.5,53	Doppler [Hz]	10,50,100

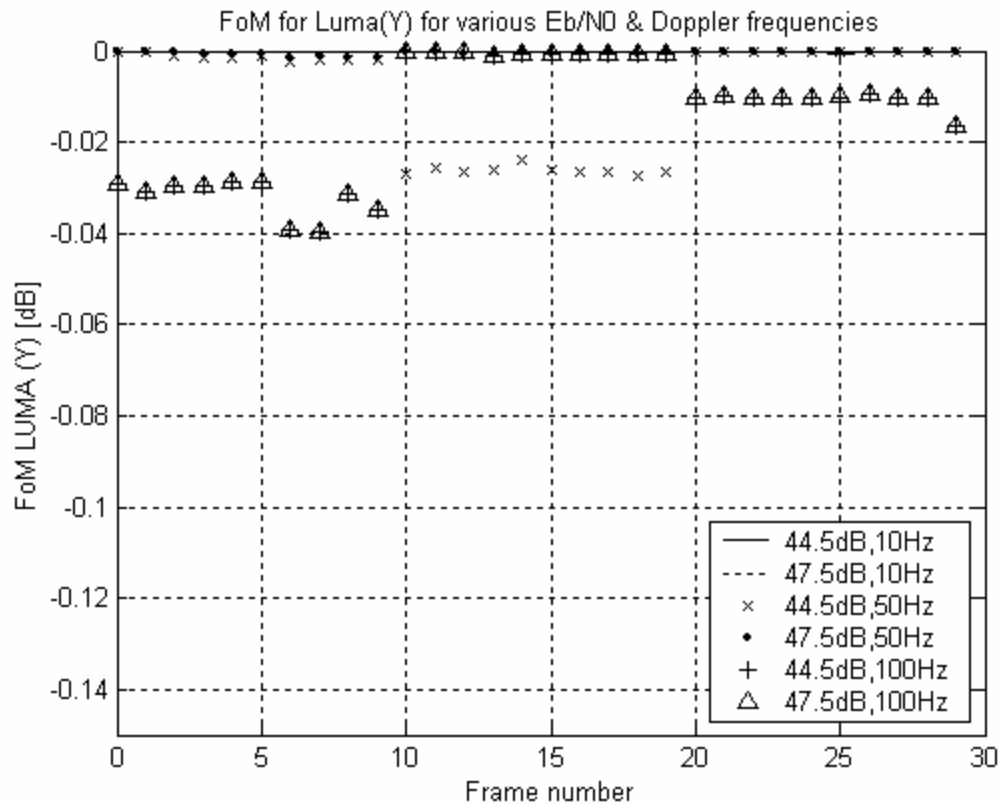


Fig. 4.12. FoM @  $F_d=10\text{Hz}, 50\text{Hz}, 100\text{Hz}$ , IDR Period=10, 6 MBs/slice for various  $E_b/N_0=44.5\text{dB}, 53\text{dB}$ .

### Experiment 5

In this experiment performances of non zero valued IDR periods and zero valued IDR periods are compared. An Error slice can propagate the errors indefinitely into future frames for a zero valued IDR period video sequence, whereas for a non zero valued IDR period, error propagation can be stopped at the boundary of each newly and correctly received IDR frame. As it has the benefit of improving the video quality at the boundary of each IDR frame, at the same it can worsen the video quality if the IDR frame is received erroneously. Hence it is necessary to compare the performance of zero valued IDR period video sequence with respect to non-zero valued IDR period video sequences transmitted over a Rayleigh fading channel. The test conditions are listed in the Table 4.11.

Table 4.11  
Experiment 5 Test Conditions

Macroblocks/Slice	6	IDR period	0,10
$E_b / N_0$ [dB]	37.5	Doppler [Hz]	50

Results from experiment 4 are chosen as the common test condition to make a fair comparison. It is clearly evident from Fig. 4.13 that performance of both techniques is similar until frame number 9. At frame number 10, the performance of non-zero valued IDR period technique dropped because of an erroneously received IDR slice. But at frame number 20 till 29, the performance of the non-zero valued IDR period technique is better than its counterpart because of a correctly received IDR slice at frame number 20. Average *FoM* is computed for both cases.

Average *FoM* from zero valued IDR period Technique: -0.0032

Average *FoM* from non-zero valued IDR period Technique: -0.0101

Subjective evaluation of the received video also suggests that the zero valued IDR period yields superior video quality compared to its counter part. But when is it advantageous to choose non –zero valued IDR period?. The Answer to this question is available in the next experiment.

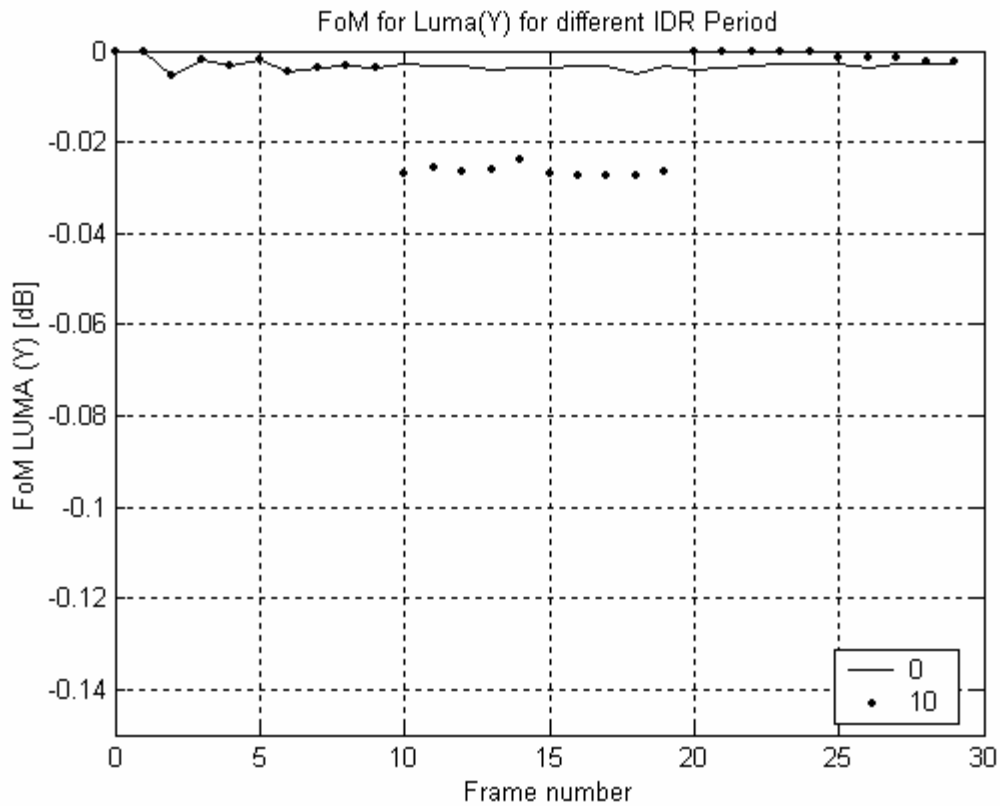


Fig. 4.13. IDR period comparison. FoM @  $F_d=50\text{Hz}$ , IDR Period=0,10, 6 MBs/slice,  $E_b/N_0=37.5\text{dB}$ .

### Experiment 6

In this experiment, test conditions are chosen such that non-zero valued IDR period source coding technique performs better than the zero valued counterpart. Table 4.12 lists the test conditions for this experiment.

Table 4.12  
Experiment 6 Test Conditions

Macroblocks/Slice	6	IDR period	0,10
$E_b / N_0$ [dB]	47.5,53	Doppler [Hz]	50,100

It can be clearly seen from the Fig. 4.14 how a non-zero valued IDR period recovers better from its earlier losses compared to its zero valued counterpart. This can be achieved only in higher values of  $E_b / N_0$ . Table 4.13 shows that the average  $FoM$  looks better for the non-zero valued IDR period technique.

Table 4.13  
Average  $FoM$  Computed for Experiment 6 Test Conditions

	Average $FoM$ [dB]
IDR Period =0, @ 47.5dB,50Hz	-0.0011
IDR Period =10, @ 47.5dB,50Hz	-0.00038
IDR Period =0, @ 53dB,100Hz	-0.0314
IDR Period =10, @ 53dB,100Hz	-0.0107

Subjective evaluation also suggests that non-zero valued IDR period source coding technique performs better at higher  $E_b / N_0$  and in addition it is more tolerant to Doppler frequencies up till 100Hz at the expense of higher data rate. This is evident from the following Fig. 4.15 of frame 20 in the Carphone video sequence. The Left part of the figure is coded using IDR period zero and it clearly distorted for  $E_b / N_0 = 53\text{dB}$  and  $Fd = 100\text{Hz}$ , whereas the right part of the figure is free from distortion.

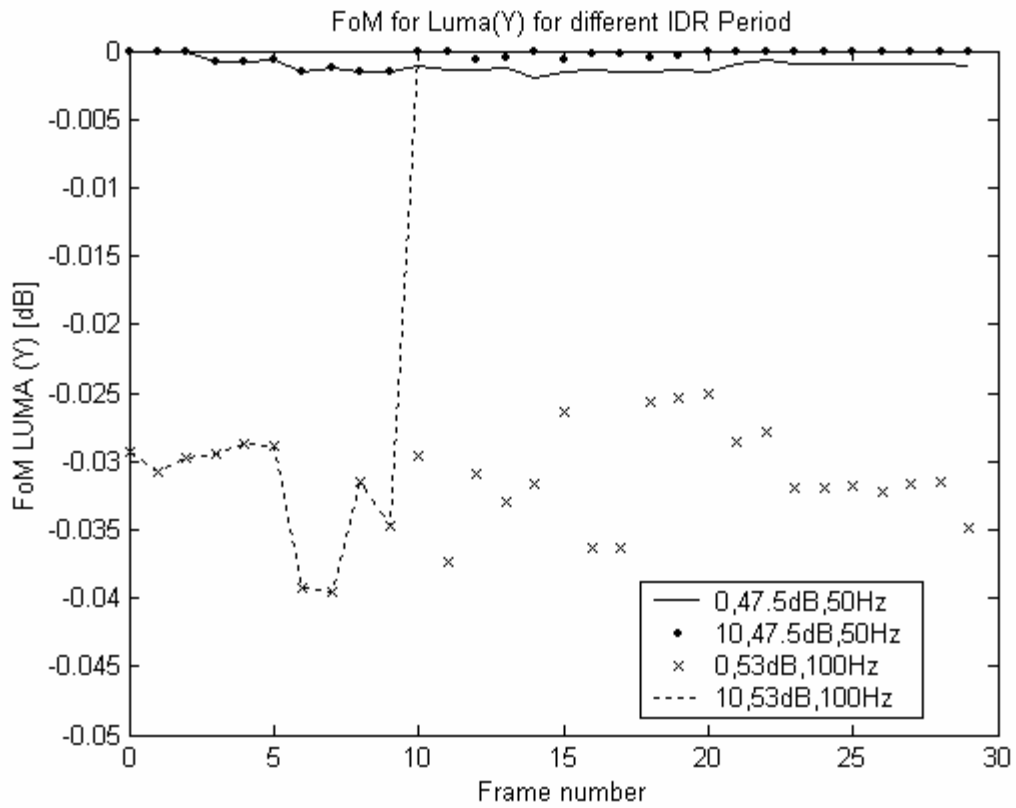


Fig. 4.14. FoM plot, IDR period =10 performing better @ higher valued  $E_b/N_0=47.5\text{dB}$ ,  $F_d=50\text{Hz}$ .

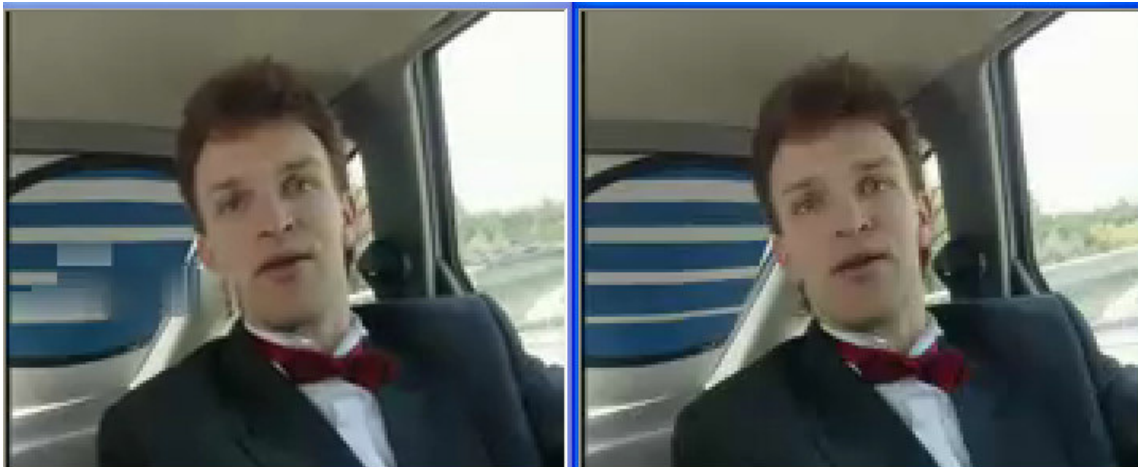


Fig. 4.15. Frame 20, Left (IDR Period=0) has distortions. Right (IDR Period=10) is distortion free.



### Experiment 7

In this experiment a single slice per picture technique is applied to each frame. In this technique, a lost slice results in complete loss of a frame. Error concealment copies the content of the previous frame into the current frame in case of frame losses. This technique is by far the least data rate consuming technique discussed so far. Test conditions are listed in the Table 4.14. Fig. 4.16 below shows the performance of this technique for various  $E_b / N_0$  and  $Fd$ .

Table 4.14  
Experiment 7 Test Conditions

Macroblocks/Slice	99	IDR period	0
$E_b / N_0$ [dB]	37.5,44.5	Doppler [Hz]	10,50

Simulation results for  $Fd = 100$  suggest that the very first IDR frame is lost, and hence there is no video signal decoded at the receiver. Subjective results also indicates that video quality is fine at  $E_b / N_0 = 44.5\text{dB}$  and  $Fd = 50\text{Hz}$ , though there is a loss of one frame. This agrees with the objective measure shown in the graph. A dip indicates that there is a frame loss. There is one lost frame at frame number 9 for the  $E_b / N_0 = 44.5\text{dB}$  and  $Fd = 50\text{Hz}$  case.

### Experiment 8

In this experiment, the three source coding features discussed in experiment 3, 4 and 7 are compared. Test conditions for this experiment are listed in the Table 4.15. The average  $FoM$  computed from simulation clearly shows that zero valued IDR period with

multiple slices per picture clearly outscores the rest of the techniques by a huge margin. It is shown in Table 4.16.

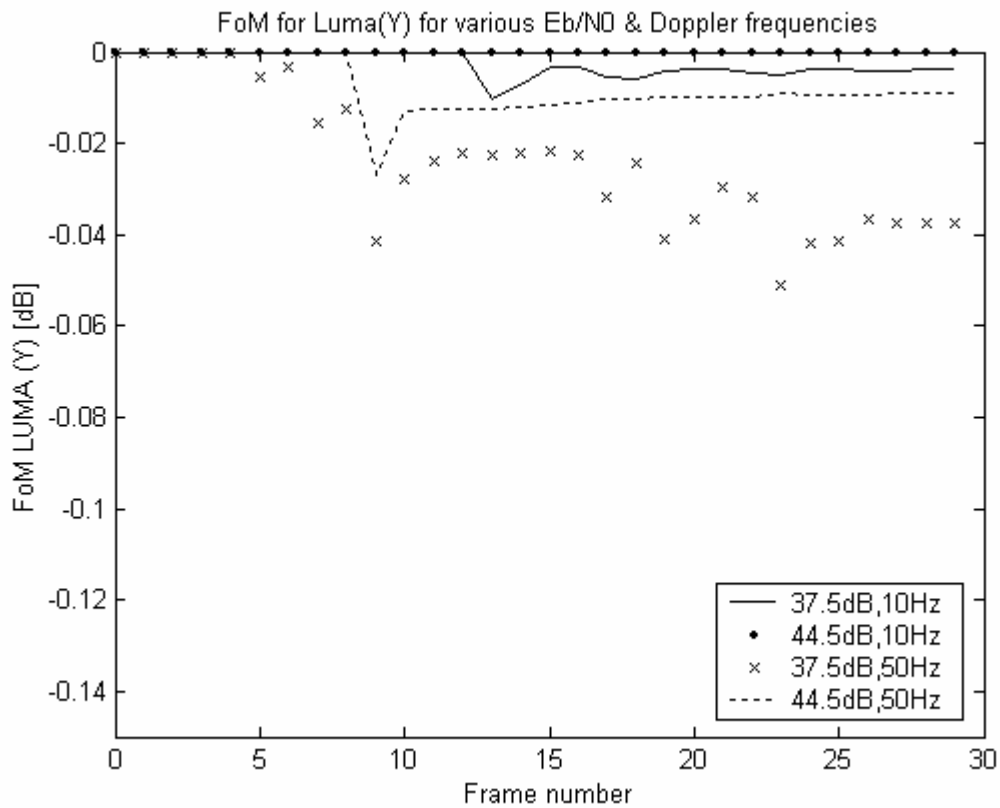


Fig. 4.16. FoM plot, Single slice/picture performance @  $E_b/N_0=37.5\text{dB}, 44.5\text{dB}, F_d=10\text{Hz}, 50\text{Hz}$ , IDR period =0.

Table 4.15  
Experiment 8 Test Conditions

Macroblocks/Slice	6,99	IDR period	0,10
$E_b / N_0$ [dB]	37.5,44.5	Doppler [Hz]	50

It can be concluded that a video signal coded with multiple slices per picture and zero valued IDR period, transmitted over a Rayleigh fading channel with  $E_b / N_0 = 37.5\text{dB}$

and  $F_d = 50\text{Hz}$  yields a good video quality at the receiver in an uncoded wireless transmission system. This can be verified from the following graph shown in Fig. 4.17.

Table 4.16  
Average  $FoM$  Computed for Experiment 8 Test Conditions

	Average $FoM$ [dB]
6MBs/slice, IDR Period =0, @ 37.5dB,50Hz	-0.0032
6MBs/slice, IDR Period =10, @ 44.5dB,50Hz	-0.0092
99MB/slice, IDR Period =0, @ 44.5dB,50Hz	-0.0079

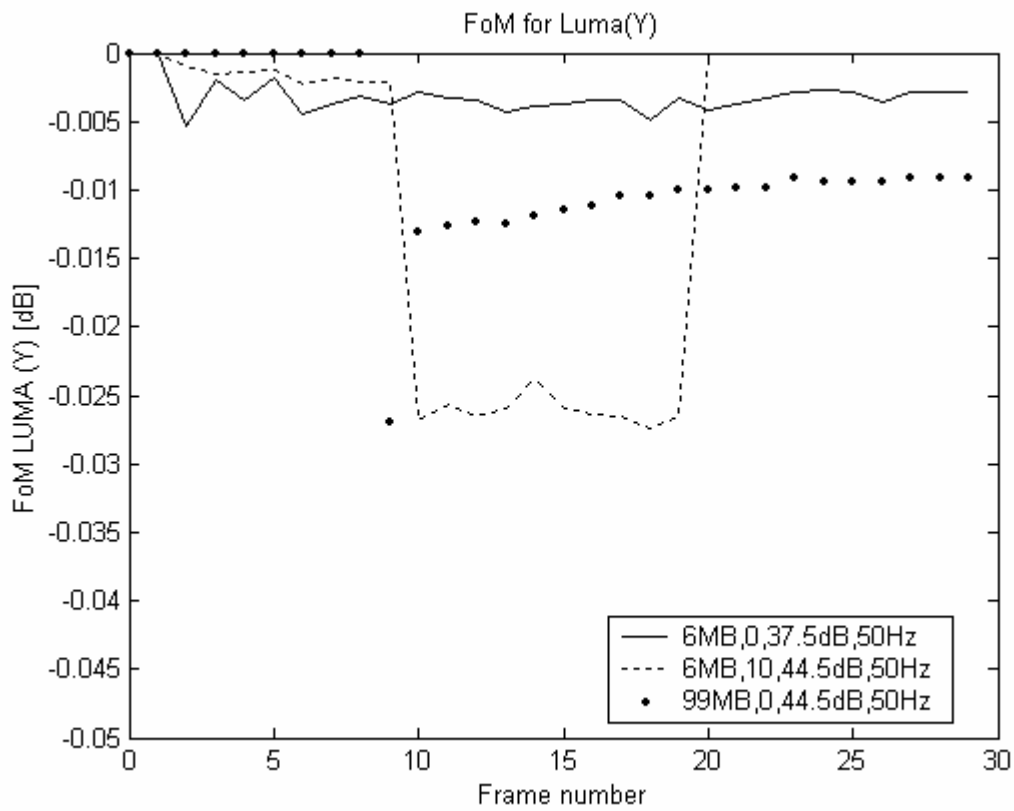


Fig. 4.17. Comparison between (1) multiple slice/picture, IDR period =0,  $E_b/N_0=37.5\text{dB}$ ,  $F_d=50\text{Hz}$ ; (2) multiple slice/picture, IDR period =10,  $E_b/N_0=44.5\text{dB}$ ,  $F_d=50\text{Hz}$ ; (3) single slice/picture, IDR period =0,  $E_b/N_0=44.5\text{dB}$ ,  $F_d=50\text{Hz}$ .

### Experiment 9

In this experiment the effect of varying RTP packet sizes on received video quality is analyzed. Due to the fixed length RTP Packetization scheme, a single NALU packet can be broken in to many fixed length RTP packets. Typically zero bits are padded to the last RTP packet. This zero padding overhead is analyzed for various RTP packet sizes. The test conditions followed in this experiment are listed in the Table 4.17.

Table 4.17  
Experiment 9 Test Conditions

Macroblocks/Slice	6	IDR period	0
$E_b / N_0$ [dB]	37.5	Doppler [Hz]	50

Typically RTP packet sizes are negotiated during the video call setup, and an optimum RTP packet size is chosen based on the available network bandwidth and the selected source coding features. Although the intention of this research is not to come up with the optimum packet size for every case, at least for completeness sake of this research, one case listed in the Table 4.17 is considered for the analysis.

Padding overhead which is expressed in Kbps is plotted against various RTP packet sizes in the Fig. 4.18. It is interesting to note that it follows a linear relationship. It is also clearly evident from Fig. 4.18 that a 50 Byte RTP packet size yields the least padding overhead among the RTP packet sizes compared.

Fig. 4.19 shows relative performance expressed in terms of  $FoM$  for various RTP packet sizes. It can be inferred from the graph, that although most of the packet sizes yield a similar pattern, the RTP packet sizes of 100 bytes and 200 bytes perform better in terms of objective video quality performance compared to other RTP packet sizes. From Fig. 4.18 and Fig. 4.19, an RTP packet size of 100 bytes can be chosen as a compromise between padding overhead and video quality.

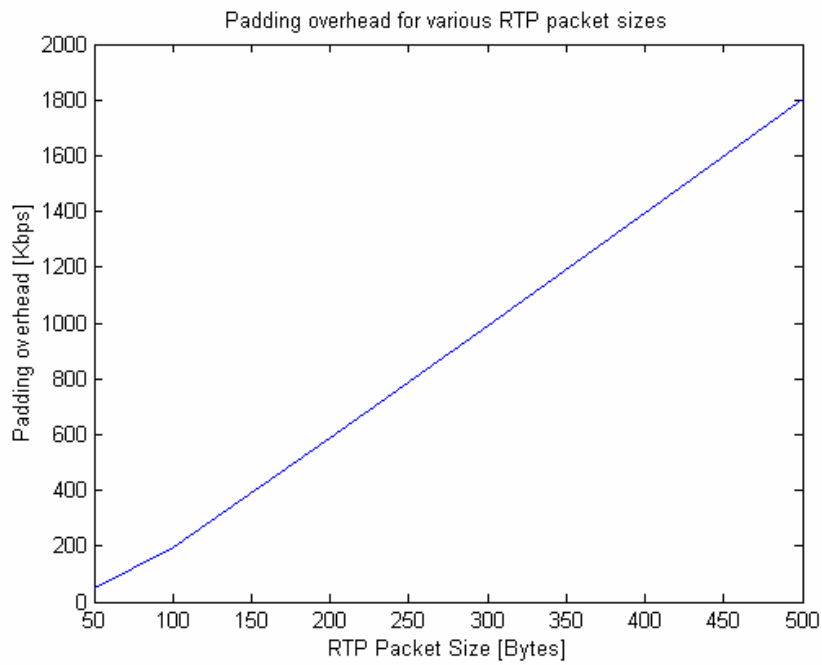


Fig. 4.18. Padding overhead [Kbps] is plotted against various RTP packet sizes.

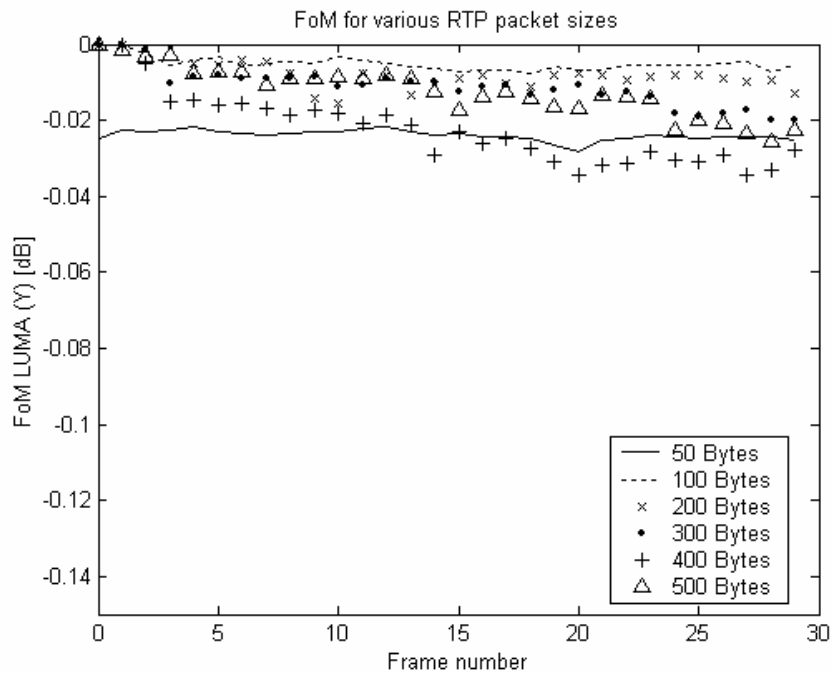


Fig. 4.19. FoM for various RTP packet sizes is compared.

### *Experiment 10*

Although the experiments considered so far are applicable only to an uncoded wireless system, the inferences from these experiments could be seamlessly extended to a coded wireless system. It is observed from the results of Experiment 8, that a video signal coded with multiple slices per picture and zero valued IDR period, transmitted over a Rayleigh fading channel with  $E_b / N_0 = 37.5\text{dB}$  and  $Fd = 50\text{Hz}$  yields a good video quality at the receiver in an uncoded wireless transmission system. By using advanced channel coding techniques and diversity techniques,  $E_b / N_0$  could be reduced significantly from 37.5dB to less than 10 dB and at the same time maintaining the same BER. In order to compare these results with a channel coded wireless system, an informational theoretical approach based channel coded wireless video system with a fixed rate code could be considered.

For a typical wireless video application, the code rate ( $R_c$ ) typically ranges from 7/8 to 1/4 based on the channel conditions. From Shannon's channel coding theorem, the channel capacity for a Gaussian channel is given by,

$$C = (1/2) * \log(1 + SNR) \text{ bits / channel use.} \quad (4.3)$$

The above equation could be used to obtain the threshold  $SNR$  that achieves the channel capacity for the hypothetical wireless system considered. For a BPSK modulated system, assuming the symbol rate ( $R_s = 1/T_s$ ) is the same as the bandwidth  $B$  of the channel, where  $T_s$  is the symbol period,  $SNR$  of the channel can be equated to the  $E_b / N_0$  of the channel. Then the equation 4.3 becomes,

$$C = (1/2) * \log(1 + E_b / N_0) \text{ bits / channel use} \quad (4.4)$$

Assuming a channel capacity achieving code with rate  $R_c = 7/8$ ,

$$7/8 = (1/2) * \log(1 + E_b / N_0) \text{ bits / channel use} \quad (4.5)$$

Solving this equation, yields

$$E_b / N_0 \text{ thresh} = 3.73 \text{ dB.} \quad (4.6)$$

Hence if the average SNR of a RTP packet is below this threshold, then the packet can be discarded as an error packet. In Fig. 4.20 the packet error rate is plotted against the various  $E_b / N_0$  values. It is clearly evident that from  $E_b / N_0 = 8$  dB onwards, the coded system can be used to transmit a video signal error free over a wireless fading channel. Fig. 4.21 depicts the video quality performance for the test conditions shown in the Table 4.18.

Table 4.18  
Experiment 10 Test Conditions

Macroblocks/Slice	6	IDR period	0
$E_b / N_0$ [dB]	7, 6.5, 6, 5.5, 5, 4	Doppler [Hz]	100

It can be clearly seen from the Fig. 4.21, that  $FoM$  is very close to the zero dB line for  $E_b / N_0 = 7$ dB, 6.5dB and 6dB, indicating that good video quality can be achieved by using advanced channel coding schemes under lower  $E_b / N_0$  values. However the video quality degrades rapidly for lower values of  $E_b / N_0$  less than 5.5dB. Hence it can be concluded that advanced channel coding schemes such as Turbo Codes, LDPC codes and convolutional codes with puncturing can indeed be used in wireless video applications to achieve superior video quality performance under lower  $SNR$  conditions.

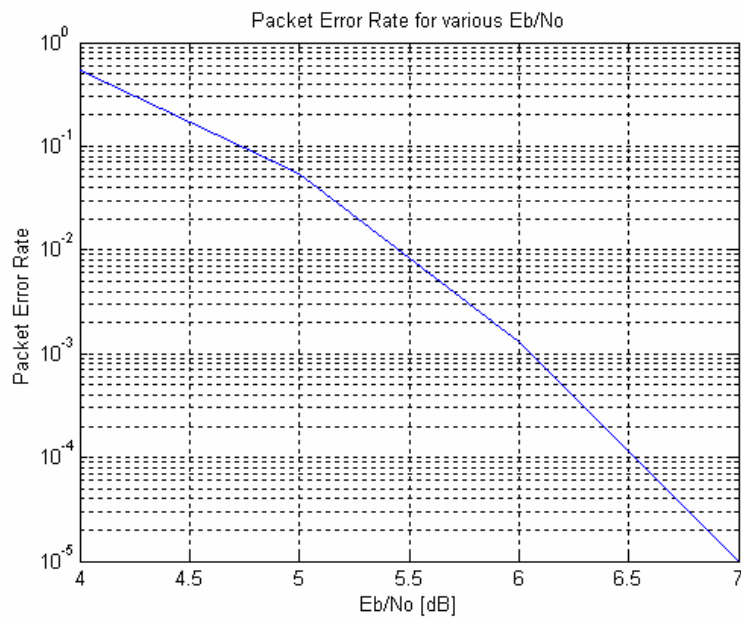


Fig. 4.20. Packet Error Rate for various Eb/No.

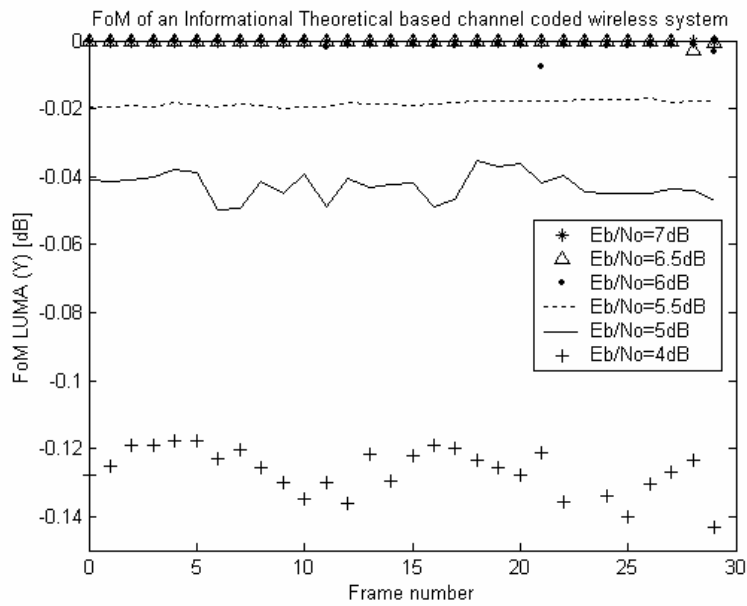


Fig. 4.21. FoM of an informational theoretical based channel coded wireless system for a video signal transported with  $E_b/N_0 = 7$ dB, 6.5dB, 6dB, 5.5dB, 5dB & 4dB.



## CHAPTER V

### HYBRID SOURCE CODING FOR VIDEO TRANSMISSION OVER RAYLEIGH FADING CHANNELS

#### A. Introduction

In this chapter, hybrid source coding for video transmission over Rayleigh fading channels is considered. Hybrid source coding refers to combined digital and analog source coding. So analog source coding which was long time untouched is revisited. Since main focus of this research is to evaluate the video transmission quality over Rayleigh fading channels, unlike in the first part of the research where pure digital coding is applied to the video signal, in the second part of this research, combined digital and analog source coding is applied to the video signal. The intention is dual fold. Firstly, by transmitting some information in an analog way, total bandwidth can be saved. Secondly, it is also needed to evaluate whether transmitting in an analog way has any effects on received video quality. In other words, received video quality must be compared between the pure digital coding versus hybrid source coding and a conclusion must be arrived about which is better. Basically, is it advantageous to do hybrid coding on a video signal transmitted on a Rayleigh fading channel. The rest of the chapter is organized as follows. Section B will introduce the system setup. Analog source coding is presented in Section C followed by an experimental setup and results in Section D.

#### B. System Setup

The system setup for pure digital coding is discussed in the previous chapter. To recapitulate, a video signal is encoded by an H.264 Encoder, digitally modulated using BPSK modulation and sent over the Rayleigh fading channel. Similarly in hybrid coding, there are two branches, a digital coding branch and an analog coding branch.

Information that needs to be sent in the respective branches must be identified first. In the digital coding branch, similar to pure digital coding, a video signal is encoded by an H.264 encoder first and then the information that is regarded for digital coding is BPSK modulated and sent over the Rayleigh fading channel. At the receiver end, received symbols are demodulated using a BPSK demodulator and the demodulated bits are supplied to an H.264 decoder for video decoding.

In encoding a video frame in the H.264 encoder, some information such as DCT coefficients can be modulated using analog modulation. In this research, DCT coefficients are Pulse Amplitude Modulated (PAM) (continuous in amplitude) and then transmitted over the Rayleigh fading channel. At the receiver, the received pulses are demodulated and then the demodulated DCT coefficients are fed to an H.264 decoder. The H.264 decoder integrates the inputs from an analog and digital channel seamlessly. An analog channel refers to the wireless channel carrying PAM modulated data and a digital channel refers to the wireless channel carrying the BPSK modulated data. The following section will present analog source coding techniques.

### **C. Analog Source Coding**

Before the data is PAM modulated, it is necessary to identify which data must be sent in the digital channel and in the analog channel. Among all parameters encoded, DCT coefficients consume almost 50% of the encoded bits. Since one of the intentions of this research is to save bandwidth by sending it in an analog channel, the DCT coefficients being large in quantity can be transmitted in an analog channel. In the following paragraphs, two analog source coding techniques will be presented.

### *$\beta$ Coding of DCT Coefficients*

A block diagram showing different functional units of this technique is shown in Fig. 5.1 and Fig. 5.2. The video signal is processed in units of macroblocks. Each macro block or sub macroblock is either intra or inter predicted. The predicted signal obtained from the above prediction, is subtracted from the original signal to obtain a residual signal or error signal. The residual signal is transformed using a DCT transform. For example, in a 4 x 4 DCT transform, 4 x 4 input residual block is transformed to yield 1 DC coefficient and 15 AC coefficients. In pure digital coding, these coefficients are first quantized, scaled and are represented in pairs of (runs of preceding zeros, level of a DCT coefficient) runs and levels and are finally converted to a bitstream using entropy coding techniques. In the reconstruction path, quantized DCT coefficients are first unquantized, rescaled and inverse transformed to yield a residual signal. This residual signal is added back to the predicted signal and the final output is filtered to yield the reconstructed video signal. In this analog source coding technique, some percentage of each DCT coefficient value is sent in the analog channel. For example, if the value of a DC coefficient is say 150. If value 37.5 is PAM modulated and sent in analog channel, and remaining  $150-37.5=112.5$  is BPSK modulated and sent in digital channel, then 25% of a DCT coefficient is being analog modulated and remaining 75% of a DCT coefficient value is being digital modulated can be inferred.

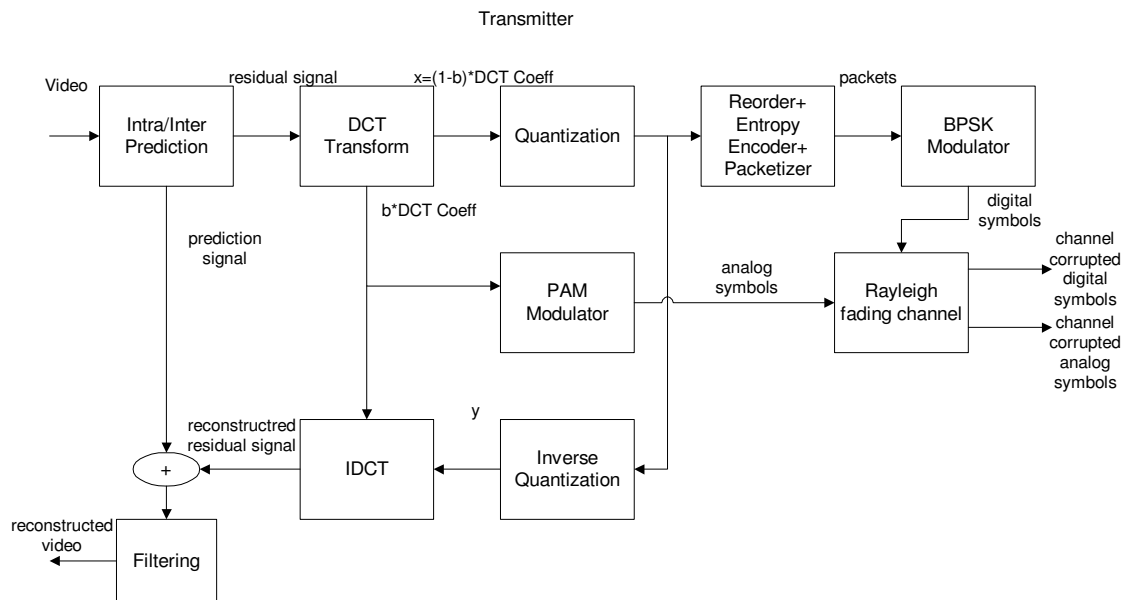


Fig. 5.1. Block diagram showing the transmitter of the hybrid scheme: Beta coding of DCT coefficients.

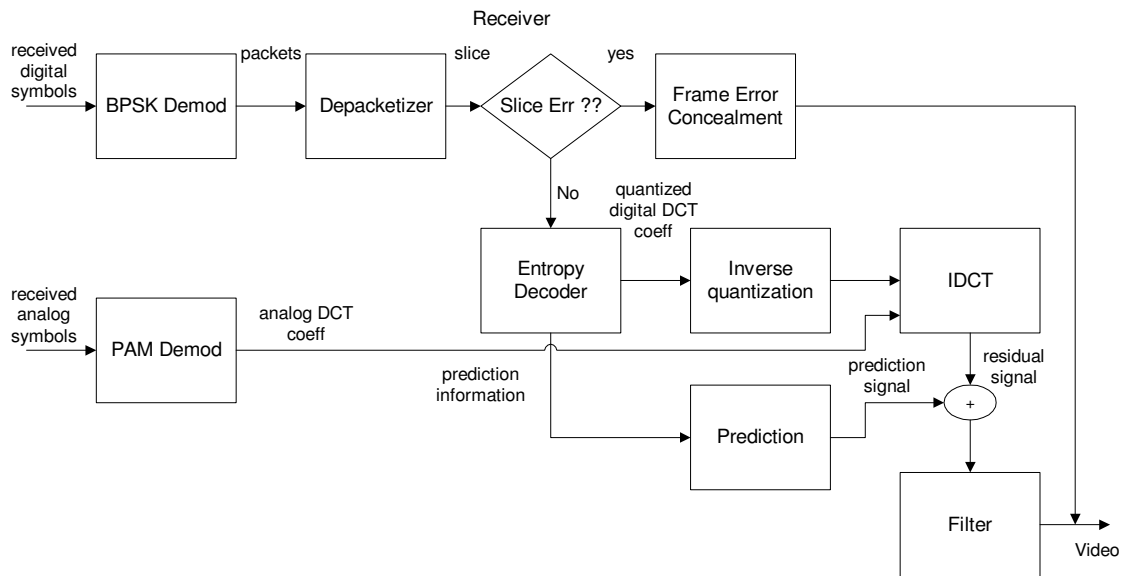


Fig. 5.2. Block diagram showing the receiver of the hybrid scheme: Beta coding of DCT coefficients.

Lets assume  $\beta$  % of a DCT coefficient is analog modulated and remaining  $100 - \beta$  % is digital modulated.

$$DCT = DCT_a + DCT_d \quad (5.1)$$

Where,

$DCT$  is value of a DCT coefficient

$DCT_a = \beta * DCT / 100$ , is the analog component of a DCT coefficient

$DCT_d = (100 - \beta) * DCT / 100$ , is the digital component of a DCT coefficient.

In the forward path,  $DCT_a$  are represented as pulse amplitudes and sent.  $DCT_d$  goes through a similar digital encoding techniques that was discussed in the previous paragraph. Let  $DCT_d^q$  denote a scaled and quantized DCT coefficient. In the reconstruction path,  $DCT_d^q$  is unquantized, rescaled and combined with  $DCT_a$ . The combined DCT coefficient  $DCT_{recon}$  is inverse transformed and then combined with the predicted signal and finally filtered to yield a reconstructed signal. This is modeled in the following equation,

$$DCT_{recon} = DCT_a + DCT_d^{\wedge} \quad (5.2)$$

Where,  $DCT_d^{\wedge}$  is unquantized and rescaled version of  $DCT_d^q$ .

The Decoder at the receiver follows a similar procedure of the reconstruction path of the encoder, except that these DCT coefficients are now corrupted by the channel. Let  $DCT_d^r$  denote the entropy decoded, unquantized and rescaled DCT coefficient.  $DCT_d^r$  is combined with the received  $DCT_a^r$  from the analog channel to yield  $DCT_r$  shown below in the equation,

$$DCT_r = DCT_a^r + DCT_d^r \quad (5.3)$$

The combined DCT coefficient  $DCT_r$  is inverse transformed and then combined with the predicted signal to yield the decoded signal.

By combining the analog component of a DCT coefficient with the digital component, quantization noise is greatly reduced. If  $\beta = 100\%$ , then perfect reconstruction can be obtained. Hence better reconstructed video quality is obtained compared to pure digital source coding. This leads to multiple benefits, firstly better reconstruction of video frame implies less error between the original signal and the reconstructed signal. Secondly, since reconstructed frames are used as reference frames, inter prediction of further frames will result in lower energy residual signal yielding to fewer bit allocation for DCT encoding thereby saving some bandwidth in digital encoding. In an error free channel, decoded video quality of hybrid coding is superior to pure digital encoding. Fig. 5.3 shows the difference in video quality of frame 1 of the Carphone video sequence.

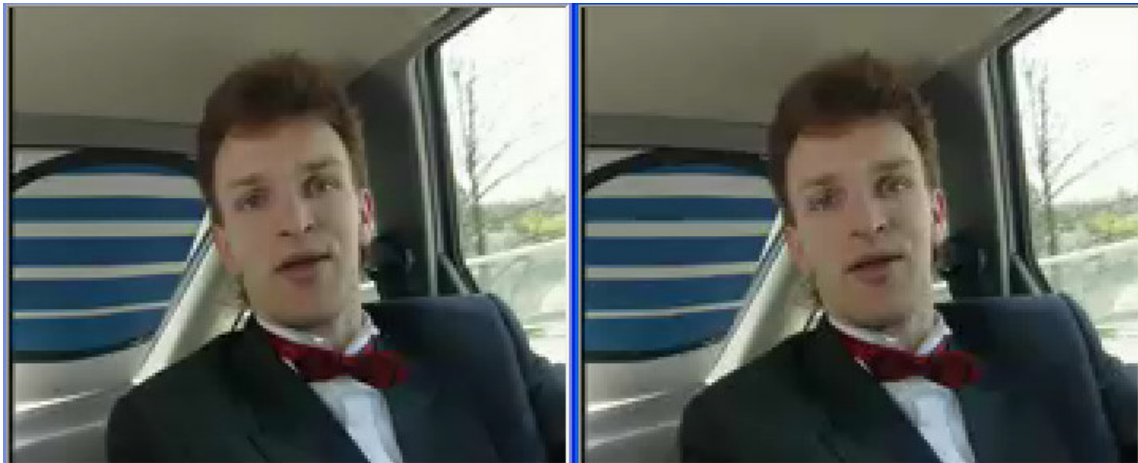


Fig. 5.3. Left picture (Hybrid Beta coding of DCT coefficients) & Right picture (pure Digital coding) in an error free channel.

It is observed that by not transmitting the analog component of the DCT coefficients for inter frame, not only saves bandwidth but also does not introduce any

perceptible degradations in the video quality. Hence it is enough to send the analog component of DCT coefficients only for Intra frames, while the coefficients are not transmitted for Inter frames, thereby saving lots of bandwidth. If a QCIF video format is considered for example, with a frame rate of 30 frames per second, the analog baseband bandwidth requirement is  $99 \text{ macroblocks} * 256 \text{ pulses per macroblock} = 25344 \text{ pulses}$ . If pulse bandwidth is assumed to be the same as the symbol rate, then the analog baseband bandwidth is 25344 Hz. The same pulse shape can be used in digital modulation. The total bandwidth required for coding a carphone sequence for 30 frames using hybrid coding is 127Khz (102Khz + 25Khz) and whereas 160 KHz is required to code using pure digital coding, thereby suggesting advantages of using hybrid coding in an error free scenario. Simulation results are available in the next section showing the total bandwidth savings for one of the scenarios considered. Experimental results on the effects of a Rayleigh fading channel on a hybrid encoded video bitstream/pulses for various scenarios are available in the next section. In the next few paragraphs, analog source coding technique 2 will be discussed.

#### *Hybrid Coding by DCT ordering*

In this technique DCT coefficients are ordered according to their level of importance. DCT coefficients are first ordered in zigzag scan order. Zigzag scan order will order DCT coefficients in the decreasing order of importance. In 4 x 4 transform, there are 16 DCT coefficients and out of which first 8 coefficients in zigzag scan order are digital encoded and the remaining 8 coefficients are transmitted in an analog fashion. The block diagrams describing the functional units of this technique are shown in Fig. 5.4 & Fig. 5.5 below.

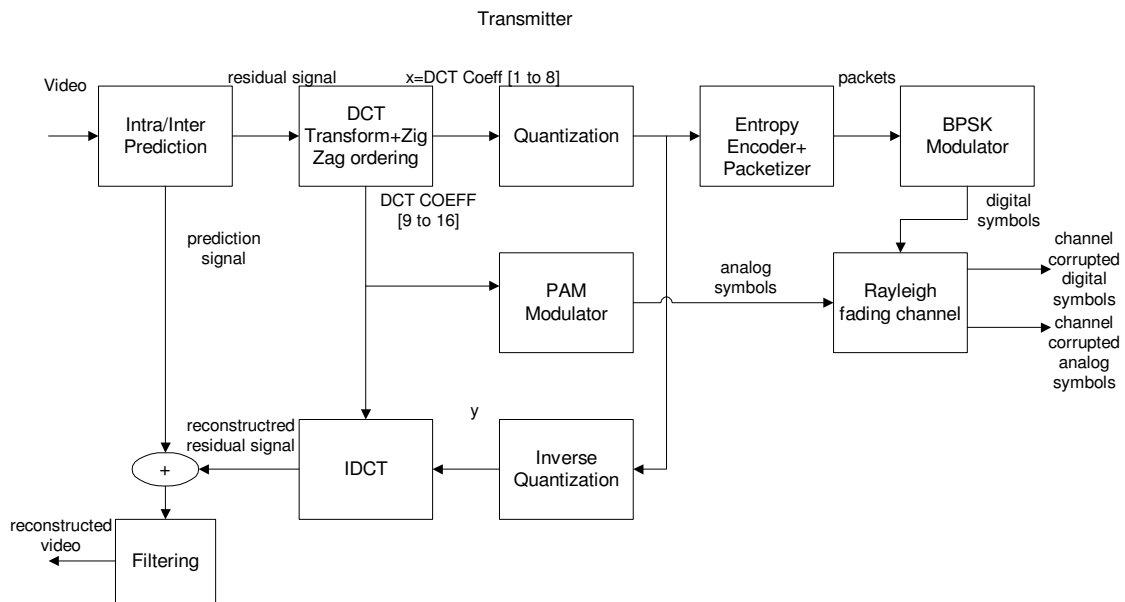


Fig. 5.4. Block diagram showing the transmitter of the hybrid scheme: DCT ordering.

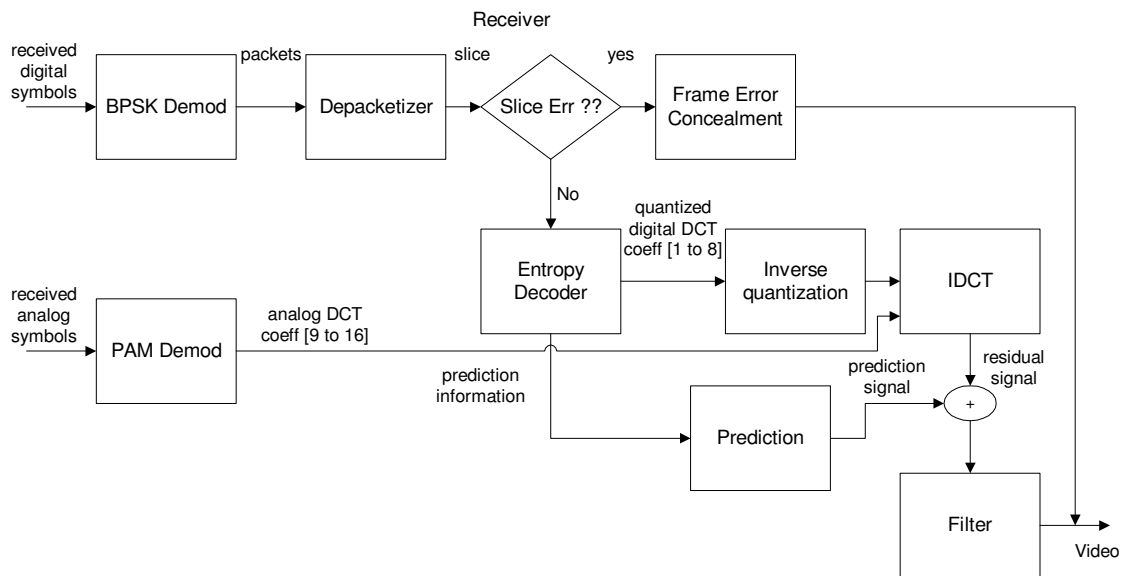


Fig. 5.5. Block diagram showing the receiver of the hybrid scheme: DCT ordering.

Let  $DCT_{1..8}$  denote the first 8 DCT coefficients arranged in zigzag scan order.

Let  $DCT_{9..16}$  denote the last 8 DCT coefficients arranged in zigzag scan order. At the



transmitter,  $DCT_{1...8}$  is first quantized, scaled and finally encoded using entropy coding and sent as a bit stream in the digital channel, whereas  $DCT_{9...16}$  is sent in an analog channel. Let  $DCT_{1...8}^q$  denote the quantized first 8 DCT coefficients. In the reconstruction path of the encoder,  $DCT_{1...8}^q$  is first un-quantized, and then rescaled to yield  $DCT_{1...8}^{\wedge}$ .  $DCT_{1...8}^{\wedge}$  and  $DCT_{9...16}$  are rearranged in a 4 x 4 matrix and an inverse DCT transformation is applied to this 4 x 4 matrix to yield the reconstructed residual block which is then added to the predicted block to yield a 4 x 4 video block.

A similar operation that is carried out in the reconstruction path of the encoder is also carried out in the decoder with the received  $DCT_{1...8}^r$  and  $DCT_{9...16}^r$  coefficients, where  $DCT_{1...8}^r$  and  $DCT_{9...16}^r$  refers to DCT coefficients that are impacted by the digital channel and analog channel respectively.

For the same reason that was explained in the previous technique, it is only necessary to send DCT coefficients in an analog channel during Intra frames. During inter frames, nothing is transmitted in the analog channel, thereby saving bandwidth. If QCIF video format is considered for example, with a frame rate of 30 frames per second, analog baseband bandwidth requirement is 99 macroblocks \*(8 pulses per 4 x 4 block)\*16 blocks per macroblock = 12672 pulses. If the pulse bandwidth is assumed to be the same as the symbol rate, then the analog base band bandwidth is 12672 Hz. This technique needs only half the bandwidth requirement of technique 1. Simulation results are also available in the next section showing total bandwidth savings for one of the scenarios considered. Experimental results on the effects of Rayleigh fading channel on this hybrid encoded video bitstream/pulses for various scenarios are presented in the next section.

## D. Experimental Results

H.264 video codec version JM9.8 is used in the following simulations. RTP packetization schemes, CRC computation and frame erasure concealment that was discussed in the previous chapter also applies here. A Rayleigh fading channel based on the time domain method is simulated in MATLAB. Physical layer modulation and demodulation for the analog and digital channels is done in MATLAB. Table 5.1 lists some common test conditions that are used in all the simulations/experiments. Table 5.2 lists test conditions that can vary between different experiments.

Table 5.1  
Hybrid Coding: Common Test Conditions

Video Sequence	Carphone	Reference Frames	5
Frame Rate	30 fps	RD Optimization	Off
Image Format	QCIF	Frames Encoded	30
Hadamard	Off	YUV Sampling	4:2:0
MV Resolution	¼ pel	Symbol Mode	UVLC
B Frames	No	16 x 16 transform	Disabled
16 x 16 intra MB prediction	Disabled	Macroblocks/Slice	6
IDR period	0	Channel	Rayleigh Fading
Digital Modulation	BPSK	Analog modulation	PAM

Table 5.2  
Hybrid Coding: Variable Test Conditions

$\beta$	0,50,100	Doppler [Hz]	10, 50 or 100
$E_b / N_0$ [dB]	33.5,37.5, 44.5,47.5,53	Hybrid coding Technique	$\beta$ coding/ DCT ordering

The  $FoM$ , which is described in the previous chapter is used here as an objective metric to evaluate the received video quality. Since Hybrid coding consists of an analog channel and digital channel, proper care must be taken such that no one channel is favored. The same realization of the Rayleigh fading process is used when simulating both analog and digital channel. The noise variance of the analog channel is appropriately computed using the following procedure. Assuming the symbol rate is the same as the bandwidth of the channel, Signal Noise Ratio ( $SNR$ ) of the analog channel is set equal to  $E_b/N_0$  of the digital channel. The noise power is computed by subtracting  $SNR$  from the signal power of the transmitted PAM symbols. The noise variance for analog channel is computed from the noise power. In the rest of chapter,  $E_b/N_0$  and  $SNR$  can be used interchangeably and they mean one and the same.

### *Experiment 1*

In this experiment, effects of varying  $E_b/N_0$  on the received video are explored. The test conditions for this experiment are presented in Table 5.3. It is evident from the graph shown in Fig. 5.6 that the channel with various  $E_b/N_0$  results in equivalent video performance at the receiver. By and large  $E_b/N_0$  does not have a major impact on the video quality performance. This fact is further strengthened by observing that there is no perceptual difference between the left and the right frame, which is shown in Fig. 5.7. The left frame is transmitted in a channel with  $E_b/N_0=33.5\text{dB}$ , whereas the right frame is transmitted in a channel with  $E_b/N_0=53\text{dB}$ .

Table 5.3  
Hybrid Coding: Experiment 1 Test Conditions

$\beta$	50	Doppler [Hz]	10
$E_b/N_0$ [dB]	33.5,37.5, 44.5,47.5,53	Hybrid coding Technique	$\beta$ coding

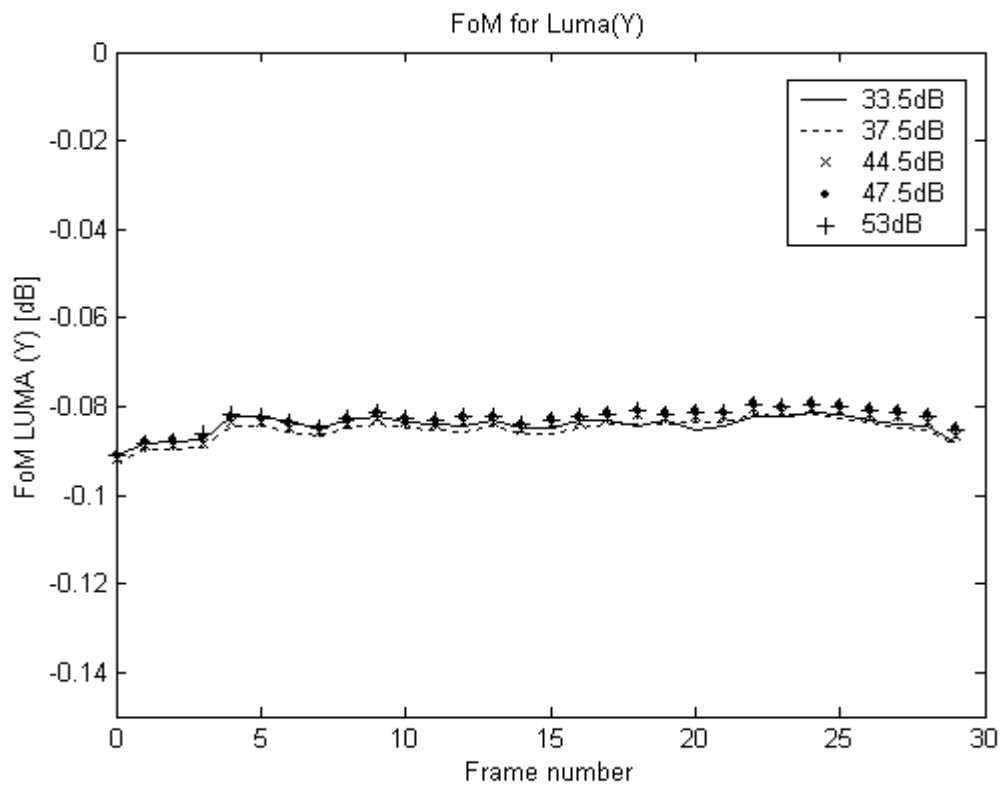


Fig. 5.6. Hybrid Beta Coding: FoM showing impact of  $E_b/N_0$  on video quality for  $F_d=10\text{Hz}$ ,  $\text{Beta}=50\%$ .

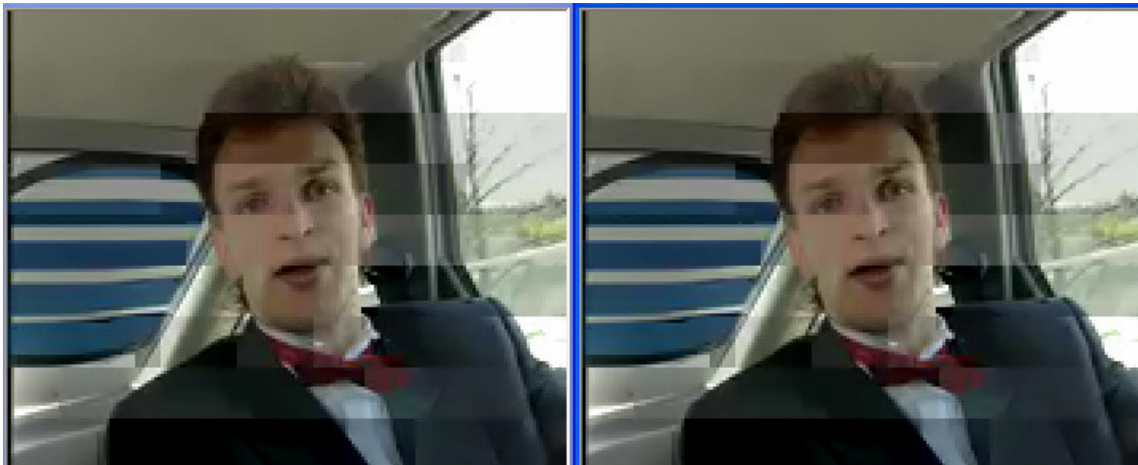


Fig. 5.7. No perceptual difference observed between Left picture ( $E_b/N_0=33.5\text{dB}$ ) and Right picture ( $E_b/N_0=53\text{dB}$ ).

It is to be noted that distortions observed due to the hybrid channel are also very different from the pure digital channel. Since Luma DCT coefficients are transmitted through an analog channel, fading and noise in the channel is manifested as uneven brightness in the received picture/frame.

### *Experiment 2*

In this experiment, the effect of Doppler frequencies on hybrid coding is analyzed. Test conditions used in the experiment are listed in the Table 5.4. It can be clearly seen from Fig. 5.8 that the quality of the video signal degrades significantly as Doppler frequency increases.

Table 5.4  
Hybrid Coding: Experiment 2 Test Conditions

$\beta$	50	Doppler [Hz]	10,50,100
$E_b / N_0$ [dB]	53	Hybrid coding Technique	$\beta$ coding

Subjective evaluation (Fig. 5.9) also indicates a very poor video quality at  $Fd = 100\text{Hz}$ . It can be concluded that Doppler frequency is a major factor impacting the performance of video in a hybrid channel. In other words, fading is the major contributor in impacting video quality performance at the receiver. Increasing  $SNR$  has negligible or no performance improvement in the video signal.

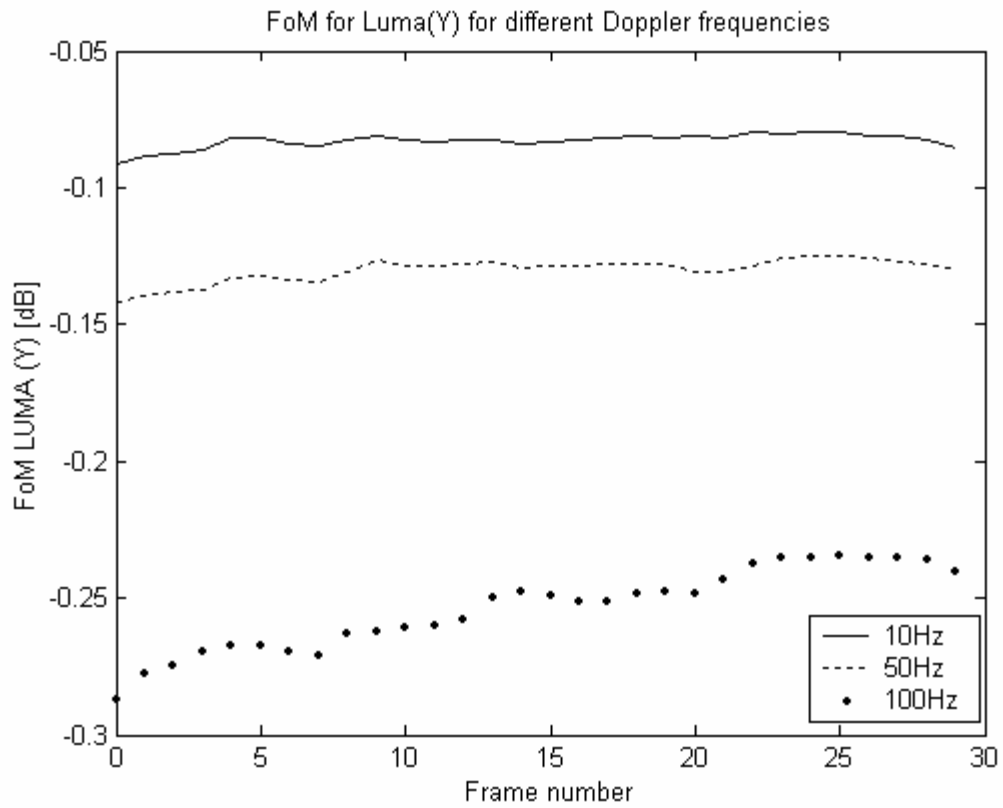


Fig. 5.8. Hybrid Beta Coding: Impact of  $F_d$  on video quality @  $E_b/N_0=53\text{dB}$  and  $\text{Beta}=50\%$ .

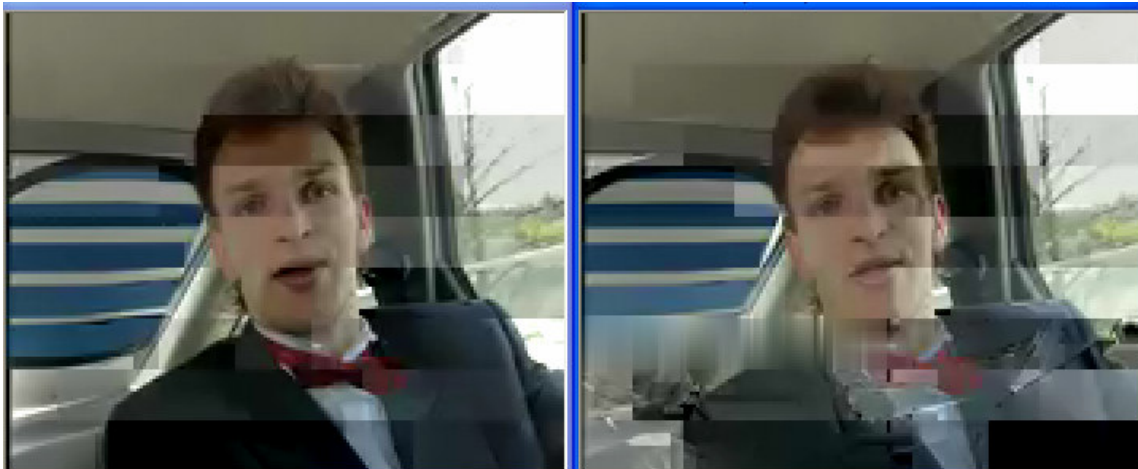


Fig. 5.9. Hybrid Beta Coding: Left picture impacted by  $F_d=10\text{Hz}$  and right picture impacted by  $F_d=100\text{Hz}$ .

### Experiment 3

The impact of changing the  $\beta$  parameter on video quality performance is analyzed here.  $\beta = 50\%$  indicates 50% of the DCT coefficient value is transmitted in both analog and digital channel.  $\beta = 100\%$  refers to transmitting all 100% of the DCT coefficient value in the analog channel. Similarly  $\beta = 0\%$  refers to transmitting all 100% of the DCT coefficient value in the digital channel, leading to pure digital coding. Test condition for this experiment is listed in the Table 5.5.

Table 5.5  
Hybrid Coding: Experiment 3 Test Conditions

$\beta$	50,100	Doppler [Hz]	10
$E_b / N_0$ [dB]	53	Hybrid coding Technique	$\beta$ coding

It can be seen from the Fig. 5.10 that transmitting all 100% of the DCT coefficient value in an analog channel yields very poor performance compared to transmitting 50% of the DCT coefficient value. This behavior is expected, because analog channel is very susceptible to fading as found in the experiment 2. Hence transmitting 100% of the DCT coefficient value makes the whole DCT coefficient exposed to fading compared to only 50% of the DCT coefficient value is exposed to fading. Hence it can be concluded that  $\beta = 50\%$  yield better video quality compared to  $\beta = 100\%$ .

### Experiment 4

Performance of Hybrid  $\beta$  coding is compared with pure digital coding in this experiment. Test conditions for this experiment are presented in the Table 5.6.

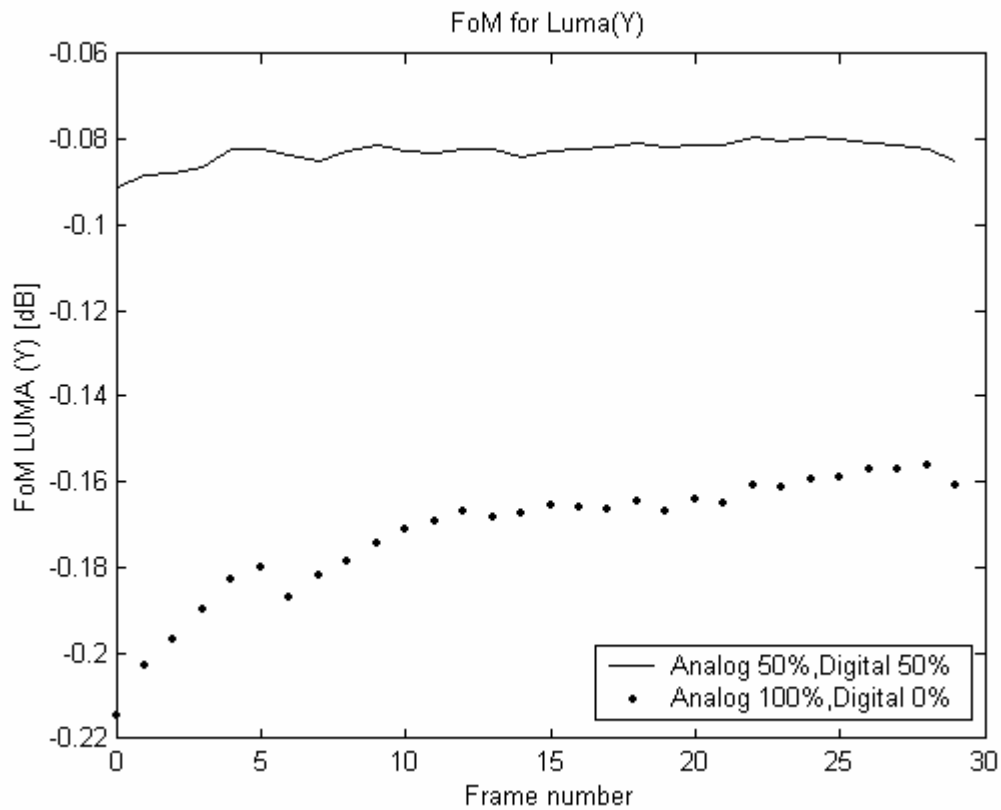


Fig. 5.10. Hybrid Beta Coding: FoM plot for Beta = 50% and Beta =100%.

Table 5.6  
Hybrid Coding: Experiment 4 Test Conditions

$\beta$	0,50	Doppler [Hz]	10
$E_b / N_0$ [dB]	44.5dB	Hybrid coding Technique	$\beta$ coding

It can be clearly seen both subjectively and objectively in Fig. 5.11 & Fig. 5.12 that the performance of hybrid coding is inferior to pure digital coding. A major part is attributed to the susceptibility of the analog channel to fading. The main reason for considering analog transmission is to save bandwidth without compromising the video



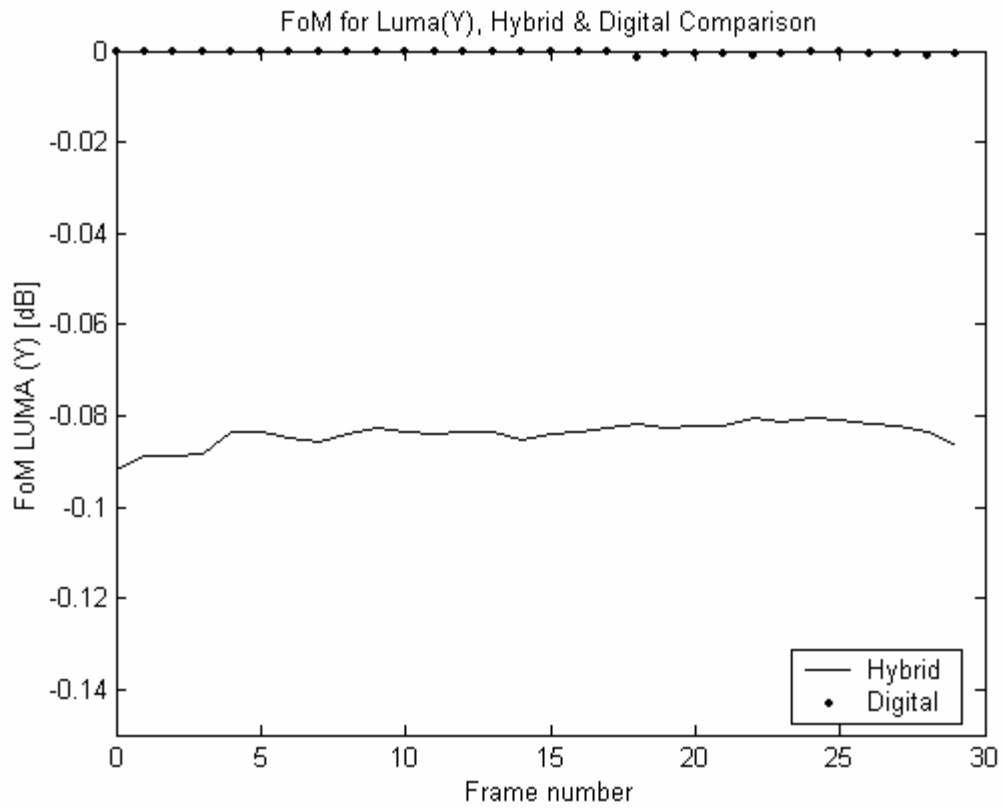


Fig. 5.11. Comparison: Hybrid Beta Coding (Beta=50%) vs Pure Digital Coding.

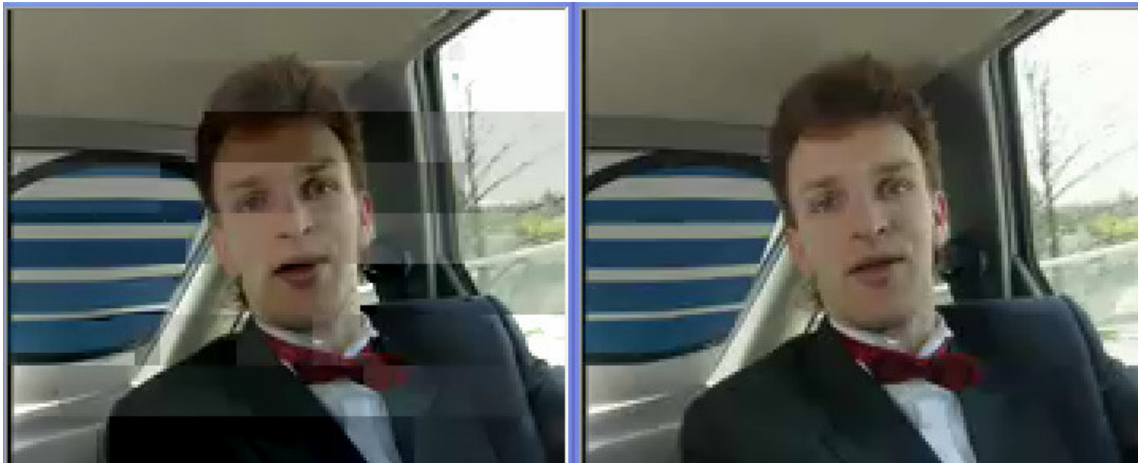


Fig. 5.12. Subjective comparison: Left picture(Hybrid Beta Coding, Beta =50% has shades of brightness) vs Right picture (Pure Digital Coding).

quality. It is observed that even transmitting DCT coefficients of a residual signal or error signal in the analog channel results in significant degradation in the video quality. Transmitting other information such as Motion vectors or prediction modes etc, in the analog channel will result in significant losses or often frame may be rendered useless. It can be concluded that hybrid coding yields inferior video quality compared to pure digital coding, although yielding some small savings in bandwidth. The total bandwidth consumed by both methods is compared in the Table 5.7.

Table 5.7  
Bandwidth Comparison: Hybrid Beta Coding,  $\beta=50\%$  vs Pure Digital Coding

Pure Digital Coding	161.26 KHz
Hybrid $\beta$ Coding	Digital (102.56Khz) + Analog (25.34) = 127.9 KHz

#### *Experiment 5*

Performance of Hybrid coding by DCT ordering is compared with the pure digital coding in this experiment. Table 5.8 lists the test conditions for this experiment.

Table 5.8  
Hybrid Coding: Experiment 5 Test Conditions

$E_b / N_0$ [dB]	44.5dB	Doppler [Hz]	10
Hybrid coding Technique	DCT ordering		

This method although it produces video quality comparable to pure digital coding, it incurs an undesirable cost of bandwidth consumption.

This is clearly evident from the Fig. 5.13 & Fig. 5.14. The total bandwidth consumed by both methods is listed in the Table 5.9.

Table 5.9  
Bandwidth Comparison: Hybrid Coding by DCT ordering vs Pure Digital Coding

Pure Digital Coding	161.26 KHz
Hybrid DCT Ordering	Digital (152.40Khz) + Analog (25.34) = 165.07 KHz

Clearly, It can be inferred that hybrid coding consumes atleast 4Khz more bandwidth than pure digital coding with no improvement in video quality.

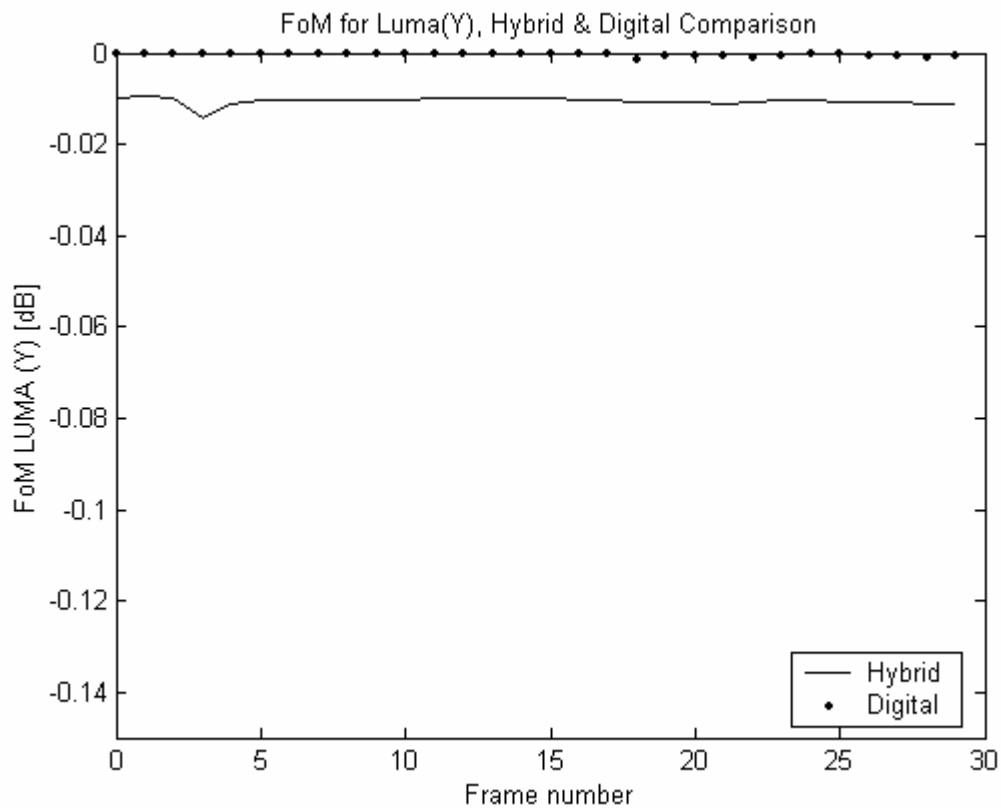


Fig. 5.13. Comparison: Hybrid Coding by DCT ordering vs Pure Digital Coding.

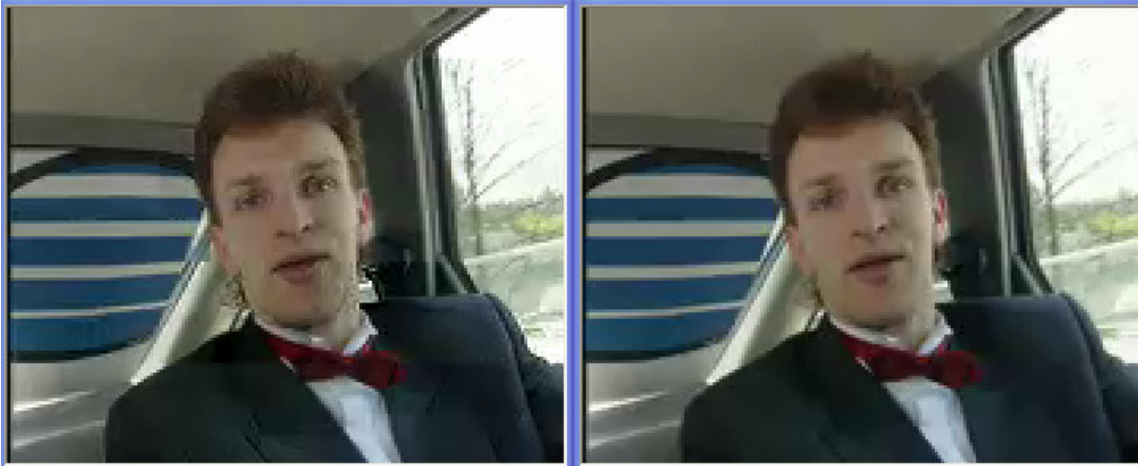


Fig. 5.14. Subjective comparison: Left picture(Hybrid Coding by DCT ordering has feeble distortions) vs Right picture (Pure Digital Coding).

## CHAPTER VI

### CONCLUSION

Video transmission over Rayleigh fading channels were analyzed for various bit error rates (BER), signal to noise ratios ( $E_b/N_0$ ) and Doppler rates. Alternative schemes such as hybrid (digital/analog) schemes were considered and their performances were compared with pure digital communication. The following paragraphs summarize the results of this research.

It is verified that video quality is impacted by changing  $E_b/N_0$  and Doppler frequencies. It is been found that for an uncoded wireless system, it is sufficient for a video signal coded at 6MBs/slice, and IDR period equal to zero, to be transmitted with  $E_b/N_0=37.5\text{dB}$  over time varying Rayleigh fading channel contributed by 50Hz Doppler frequency.

Though non-zero valued IDR period can be used to prevent propagation of errors, it is not advantageous to use this feature for  $E_b/N_0$  less than or equal to 37.5 dB or BER greater than or equal to  $5*10^{-5}$ . However for higher  $E_b/N_0$  greater than or equal to 47.5dB or BER less than or equal to  $5*10^{-6}$ , it is found that the video signal coded with non-zero valued IDR period is more robust to Rayleigh fading compared to video signal coded with the zero valued IDR period.

Video signal coded using single slice per picture is very susceptible to Rayleigh fading and yields the worst performance compared to its counterparts. Since it is desired for uncoded wireless system to be able to operate at as low  $E_b/N_0$  as possible and be robust against high Doppler frequencies, it is found that video signal coded using multiple slice per picture, with zero valued IDR period transmitted in a Rayleigh fading with  $E_b/N_0=37.5\text{dB}$  or BER equal to  $5*10^{-5}$  and Doppler frequency equal to 50Hz yields the best performance among the features considered. By using advanced coding

techniques and/or diversity techniques,  $E_b / N_0$  can be reduced to operate at BER equal to  $5 * 10^{-5}$ . Hence these results can be easily extended to coded wireless system.

It is interestingly found that, the performance of hybrid coding is not impacted by changing  $E_b / N_0$  values. In other words, the performance improvements in a hybrid system for higher  $E_b / N_0$  values are negligible. However, it can be concluded that Doppler frequency is the major factor impacting the performance of video in a hybrid channel. To summarize, video transmitted using hybrid coding is extremely susceptible to fading compared to the noise added at the receiver.

Though hybrid coding using  $\beta$  coding yields significant bandwidth savings, because of its vulnerability to fading, received video quality is found to be inferior compared to the pure digital counterpart. The savings in bandwidth did not justify inferior video quality. Hybrid coding using DCT ordering in spite of consuming more bandwidth than its pure digital counter part does not yield better received video quality. The above results are also attributed to lack of robust demodulation schemes for analog transmission, because it is very difficult or impossible to detect errors in analog source coding. Analog communication can only be used to transmit data which has negligible or no significant impact to the received video quality. But why should there be a need to transmit such information if it doesn't yield any video quality improvement. This is conflicting with the video compression research which is aimed at transmitting as less information as possible. Hence it can be concluded that combination of digital and analog video communication does not yield any better performance compared to its pure digital video communication.

## REFERENCES

- [1] I. E. G. Richardson, *H.264 and MPEG-4 Video Compression*, West Sussex: John Wiley & Sons, September 2003.
- [2] T. Wiegand, G. J. Sullivan, G. Bjontegaard, and A. Luthra, "Overview of the H.264/AVC video coding standard," *IEEE Trans. Circuits Syst. Video Technol.*, vol. 13, pp. 560-576, July 2003.
- [3] W. Jakes, Ed. *Microwave Mobile Communications*, New York: Wiley, 1974.
- [4] J. G. Proakis, *Digital Communication*, New York: McGraw-Hill, 2<sup>nd</sup> Ed., 1989.
- [5] T. Rappaport, *Wireless Communication*, New Jersey: Prentice-Hall, 2<sup>nd</sup> Ed., 2002.
- [6] S. Miller, "Wireless Communication, Spring 2005 lecture notes", Available at: <http://www.ece.tamu.edu/~smiller/Wireless/Homepage.htm>.
- [7] Y. Gong, "H.264/AVC Video Transmission over Wireless Channels," *WISICT'03*, Cancun, Mexico, January, 2004.
- [8] S. Wenger, "H.264/AVC Over IP," *IEEE Trans. Circuits Syst. Video Technol.*, vol.13, pp. 645-656, July 2003.
- [9] T. Stockhammer, M. Hannuksela, and T. Wiegand, "H.264/AVC in wireless environments" *IEEE Trans. Circuits Syst. Video Technol.*, vol.13, pp. 657-673, July 2003.
- [10] S. Zhao, Z. Xiong, and X. Wang, "Optimal resource allocation for wireless video over CDMA networks," *IEEE Transactions on Mobile Computing*, vol. 4, pp. 56-67, Jan./Feb. 2005.
- [11] Y. Shen, P. C. Cosman, L. B. Milstein, "Error Resilient Video Communication over CDMA Networks with a Bandwidth Constraint," Dept. Elec. & Comp. Engg., University of California, San Diego, USA.
- [12] L. P. Kondi, S. N. Batalama, D. A. Pados, and A. K. Katsaggelos, "Joint source/channel coding for scalable video over DS-SS multipath fading channels," *IEEE Int. Conf. Image Processing*, pp. 994-997, Oct. 2001.

- [13] D. Srinivasan, L. P. Kondi, D. A. Pados, "Scalable video transmission over wireless DS-CDMA channels using minimum TSC spreading codes", *IEEE Signal Processing Letters*, vol. 11, no. 10, pp. 836-840, Oct. 2004.
- [14] S. S. Hemami, "Robust image transmission using resynchronizing variable-length codes and error concealment," *IEEE J. Select. Areas Commun.*, vol. 18, pp. 927-939, June 2000.
- [15] G. Cote, S. Shirani, and F. Kossentini, "Optimal mode selection and synchronization for robust video communications over error-prone networks," *IEEE J. Select. Areas Commun.*, vol. 18, pp. 952-965, Dec. 2000.
- [16] U. Horn, K. Stuhlmuller, M. Link, and B. Girod, "Robust internet video transmission based on scalable coding and unequal error protection," *IEEE Trans. Image Processing*, vol. 15, pp.77-94, Sept. 1999.
- [17] Q. F. Zhu and L. Kerofsky, "Joint source coding, transport processing, and error concealment for H.263-based packet video," *Proc. SPIE VCIP*, vol. 3653, pp. 52-62, Jan. 1999.
- [18] Y. Wang and Q. Zhu, "Error control and concealment for video communication: A review," *Proc. IEEE*, vol. 86, pp. 974-997, May 1998.
- [19] V. Varsa, M. M. Hannuksela, and Y. Wang, "Non-normative error concealment algorithms," ITU-T VCEG-N62, 2001, Available at: [http://ftp3.itu.int/av-arch/video-site/0109\\_San/](http://ftp3.itu.int/av-arch/video-site/0109_San/).
- [20] G. Carle and E. W. Biersack, "Survey of error recovery techniques for IP-based audio-visual multicast applications," *IEEE Network Mag.*, vol. 11, pp. 2-14, Nov. 1997.
- [21] Y.-K. Wang, M. M. Hannuksela, V. Varsa, A. Hourunranta, and M. Gabbouj, "The error concealment feature in the H.26L test model," in *Proc. ICIP*, vol. 2, Sept. 2002, pp. 729-732.
- [22] B. Girod and N. Farber, "Feedback-based error control for mobile video transmission," *Proc. IEEE*, vol. 97, pp.1707-1723, Oct. 1999.



- [23] R. Zhang, S. L. Regunathan, and K. Rose, "Video coding with optimal inter/intra-mode switching for packet loss resilience," *IEEE Journal on Selected Areas in Communications*, vol. 18, no. 6, pp. 966-976, June 2000.
- [24] V. Stankovic, R. Hamzaoui, and Z. Xiong, "Real-Time Error Protection of Embedded Codes for Packet Erasure and Fading Channels," *IEEE Trans. Circuits Syst. Video Technol.*, vol.14, no.8, pp. 1064-1072, Aug. 2004.
- [25] Y. Shen, P. C. Cosman, and L. B. Milstein, "Video coding with fixed length packetization for a tandem channel," *IEEE Transactions on Image Processing*, vol. 15, no.2, pp. 273-288, Feb. 2006.
- [26] V. Varsa, G. Roth, T. Stockhammer, R. Sjoberg, G. Liebl, M. Karczewicz "Common test conditions for RTP/IP over 3GPP/3GPP2," ITU-T VCEG-M77.doc, 2001, Available at: [http://ftp3.itu.int/av-arch/video-site/0104\\_Aus/](http://ftp3.itu.int/av-arch/video-site/0104_Aus/).
- [27] S. Wener, M. Hannuksela, T. Stockhammer, M. Westerlund, and D. Singer, "RFC:3984 RTP payload format for H.264 Video," Internet Draft, February 2005.
- [28] J. Rosenberg and H. Schulzrine, "An RTP payload format for generic forward error correction," in RFC 2733, Dec. 1999.
- [29] P. Salama, N. B. Shroff, and E. J. Delp, "Error concealment in encoded video," in *Image Recovery Techniques for Image Compression Applications*. Norwell, M.A: Kluwer, 1998.
- [30] J. Liao and J. Villasenor, "Adaptive intra update for video coding over noisy channels," *Proc. ICIP*, vol. 3, pp. 763-766, Oct. 1996.
- [31] W. M. Lam, A. R. Reibman, B. Liu, "Recovery of lost or erroneously received motion vectors," in *Proc. ICASSP*, vol. 5, Mar: 1993, pp. 417-420.
- [32] "H.264/AVC Software Ref. Ver. JM9.8," May 2005, Available at: <http://www.iphome.de/suehring>.

## VITA

Karthik Kannan received his Bachelor of Engineering degree in electronics and communication engineering from the Bharadhidasan University, Regional Engineering College at Trichy in 1999. He entered the electrical engineering program at Texas A&M University in August 2004, and since then he has been pursuing his Master of Science degree receiving it in August 2006. His research interests include wireless communication, video and audio signal processing.

Mr. Karthik may be reached at 214, Zachry Engineering Center, Texas A&M University, College Station, Tx 77843. His email address is [kkannan@tamu.edu](mailto:kkannan@tamu.edu).